



1 **Vertical profiles of volatile organic compounds and fine particles in**
2 **atmospheric air by using aerial drone with miniaturized samplers and**
3 **portable devices**

4 Eka Dian Pusfitasari^{1,2}, Jose Ruiz-Jimenez^{1,2}, Aleksi Tiusanen¹, Markus Suuronen¹, Jesse Haataja³, Juha
5 Kangasluoma³, Krista Luoma^{3,4}, Tuukka Petäjä³, Matti Jussila^{1,2}, Kari Hartonen^{1,2*}, and Marja-Liisa
6 Riekkola^{1,2*}.

7 ¹Department of Chemistry, P.O. Box 55, FI-00014 University of Helsinki, Finland

8 ²Institute for Atmospheric and Earth System Research, Chemistry, Faculty of science, P.O. Box 55, FI-
9 00014 University of Helsinki, Finland

10 ³Institute for Atmospheric and Earth System Research, Physics, Faculty of science, P.O. Box 64, FI-00014
11 University of Helsinki, Finland

12 ⁴Finnish Meteorological Institute, P.O. Box 503, FI-00101 Helsinki, Finland

13

14 *Corresponding authors: Dr. Kari Hartonen (kari.hartonen@helsinki.fi) and prof. Marja-Liisa Riekkola
15 (marja-liisa.riekkola@helsinki.fi)

16

17 **Abstract.** The increase of volatile organic compounds (VOCs) emissions released into the atmosphere is one
18 of the main threats to human health and climate. VOCs can adversely affect human life through their
19 contribution to air pollution directly and indirectly by reacting via several mechanisms in the air to form
20 secondary organic aerosols. In this study, aerial drone equipped with miniaturized air sampling systems
21 including up to four solid-phase microextraction (SPME) Arrows and four in-tube extraction (ITEX)
22 samplers for the collection of VOCs, along with portable devices for the real-time measurement of black
23 carbon (BC) and total particle numbers at high altitudes was exploited. In total, 135 air samples were collected
24 under optimal sampling conditions in October 2021 at the boreal forest SMEAR II Station, Finland. A total
25 of 48 different VOCs, including nitrogen-containing compounds, alcohols, aldehydes, ketones, organic acids,
26 and hydrocarbons, were detected at different altitudes from 50 to 400 m above ground level with the
27 concentrations up to 6898 ng m⁻³ in gas phase and 8613 ng m⁻³ in particle phase. Clear differences in VOCs
28 distribution were seen in samples collected from different altitudes, depending on the VOC sources. It was
29 also possible to collect aerosol particles by the filter accessory attached on the ITEX sampling system, and
30 five dicarboxylic acids were quantified with the concentrations of 0.43 to 10.9 µg m⁻³. The BC and total
31 particle number measurements provided similar diurnal patterns, indicating their correlation. For spatial



32 distribution, surprisingly the BC concentrations were increased at higher altitudes being 2278 ng m⁻³ at 100
33 m and 3909 ng m⁻³ at 400 m. The measurements onboard the drone provided insights into horizontal and
34 vertical variability in BC and aerosol number concentrations above the boreal forest.

35 **Keywords:** aerial drone; miniaturized air sampling systems; solid-phase microextraction Arrow; in-tube
36 extraction; volatile organic compounds; black carbon; total particle number.

37 1. Introduction

38 The global phenomenon of climate change has attracted a huge attention in the past decades. Atmospheric
39 aerosol particles can influence the climate system directly by scattering sunlight, transmission, and absorption
40 of radiation, and indirectly by acting as nuclei for cloud formation (Hemmilä, 2020; Kim et al., 2017; Oh et
41 al., 2020). Fine aerosol particles have sizes close to the wavelength range of the visible light, and therefore
42 they are expected to have a stronger climatic impact than larger particles (Kanakidou et al., 2005). In addition,
43 the aerosol particles also give an adverse effect on air quality and human health by exposing human's
44 respiratory system to aerosol particulate matter (PM) that can get into lungs and translocate into vital organs
45 due to their tiny size (Fu et al., 2013).

46 The formation and growth process of aerosol particles have been studied by many research groups (Ahlberg
47 et al., 2017; Camredon et al., 2007; Casquero-Vera et al., 2020; Kulmala et al., 2014, 2013; Peng et al., 2021;
48 Ziemann and Atkinson, 2012). To study the particle formation in the atmosphere, it is important to assess the
49 possible sources of the atmospheric particles, for instance by the presence of volatile organic compounds
50 (VOCs). Hydrocarbons and amines e.g. have been extensively investigated either by modelling or by
51 laboratory chamber experiments to show their contribution to secondary organic aerosol (SOA) formation.
52 These VOCs, along with other thousands of organic gaseous trace species, are directly emitted from biogenic
53 and anthropogenic sources. In the atmosphere, VOCs are oxidized by reactions with atmospheric oxidants
54 such as O_3^- , OH^- , NO_3^- and Cl^- radicals to form less volatile products and further subsequently partition into
55 aerosol particle leading to SOA formation (Almeida et al., 2013; Kulmala et al., 2014; Zahardis et al., 2008;
56 Ziemann and Atkinson, 2012). The SOAs then become the major components of fine aerosol particulate
57 matter, such as PM 10 and PM 2.5 that pollutes the environment (Fermo et al., 2021; Ge et al., 2011; Kulmala
58 et al., 2014).

59 Another important component that contributes to air pollution is Black Carbon (BC), which is emitted mostly
60 as a byproduct of fossil fuel combustion and biomass burning (Hyvärinen et al., 2011). In addition, industry,



61 energy production, and domestic cooking contribute to the BC in the atmosphere (Kumar et al., 2015). BC
62 has been associated with adverse effects on human health, such as premature mortality, and also on earth
63 temperature and climate, since it absorbs solar radiation very strongly (Anenberg et al., 2012; Jacobson,
64 2010).

65 In addition to VOCs and BC, atmospheric organic acids, such as low molecular weight (LMW) dicarboxylic
66 acids are also recognized as ubiquitous aerosol constituents in the urban region. As highly water-soluble
67 compounds they have the capability to significantly enhance the hygroscopicity of aerosol particles
68 (Kanakidou et al., 2005). LMW diacids can be emitted from biomass burning, vehicular exhausts, natural
69 marine, and also produced from the atmospheric photo-oxidation of various organic precursors (Fu et al.,
70 2013; Kawamura and Sakaguchi, 1999; Rinaldi et al., 2011).

71 The condensation particle counters (CPC) are important devices for the measurement of aerosol number
72 concentrations and aerosol particle fluxes (Kangasluoma and Attoui, 2019; McMurry, 2000; Petäjä et al.,
73 2001). CPCs are commonly used in the ambient air quality monitoring to measure the number concentration
74 of airborne submicron particles with sizes down to a few nanometers (Asbach et al., 2017; Buzorius et al.,
75 1998). The conventional CPCs have generally not been used as portable devices due to their weight and size.
76 However, recently small CPCs are emerging and being deployed for example for vertical profiling on-board
77 drones (Carnerero et al., 2018; Kim et al., 2018), and other platforms (Petäjä et al., 2012).

78 In our previous research, we used reliable and versatile miniaturized air sampling (MAS) techniques, which
79 have many benefits for on-site sampling, such as small size, low sampling time, environmental friendliness,
80 easy operation and flexibility for practical applications and automation (Lan et al., 2020; Pusfitasari et al.,
81 2022; Ruiz-Jimenez et al., 2019). Solid-phase microextraction (SPME) Arrow and in-tube extraction (ITEX)
82 sampling systems have been successfully employed for the reliable collection of VOCs from ambient air
83 samples (Lan et al., 2019b, 2019a; Pusfitasari et al., 2022). Extra sampling accessories, including adsorbent
84 trap and filter accessories together with ITEX have enhanced the selectivity of the sampling system and
85 allowed the ITEX to collect only gas phase (Pusfitasari et al., 2022). After sample collection, the compounds
86 were desorbed from the samplers, separated and detected by thermal desorption (TD) gas chromatography-
87 mass spectrometry (GC-MS).

88 In this study, the sampling of VOCs and measurement of total particle number concentration and Black
89 Carbon (BC) directly at various altitudes, from 50 to 400 m, were performed using an aerial drone as the



90 platform as in our previous research (Lan et al., 2021; Pusfitasari et al., 2022; Ruiz-Jimenez et al., 2019). The
91 sampling platform contained now up to four SPME Arrows and four ITEX units, with additional portable
92 commercial BC device for BC real-time measurement and a lab-made portable CPC for total particle number
93 observation. The compositions of different fractions of the gas phase, collected by SPME Arrow and ITEX,
94 aerosol particles collected by ITEX sampling including filter accessory as well as BC and particle numbers
95 were evaluated at different altitudes and temporal variation at boreal forest SMEAR II Station in October
96 2021. In addition, the possible correlation between VOCs, BC and total particle number concentrations were
97 also clarified.

98 **2. Materials and methods**

99 **2.1. Reagent and materials**

100 Detailed information of reagents used, including their purities, is given in the supplemental information S1.
101 Empty ITEX units, DVB-PDMS and Carbon coated WR-SPME Arrow systems were purchased from BGB
102 Analytik AG (Zurich, Switzerland). TENAX-GR was purchased from Altech (Deerfield, IL, USA). The
103 mesoporous silica-based materials, the Mobil Composition of Matter No. 41 (MCM-41) and titanium
104 hydrogen phosphate-modified (MCM-41-TP) materials were synthesized via sol-gel template as described
105 in our previous publication (Lan et al., 2019a). The instructions for ITEX packing with 30 mg MCM-41-TP
106 and 60 mg Tenax-GR are described in Lan *et al.* (2019b). The preparation of MCM-41-SPME Arrow with
107 the sorbent thickness of 40 μm and length of 20 mm, is found from Lan *et al.* (2019a).

108 **2.2. Instrumentation**

109 A lab-made permeation system was employed to create an artificial gas-phase sample in the laboratory (Lan
110 et al., 2021, 2019a; Pusfitasari et al., 2022). A PAL Cycle Composer and PAL RTC autosampler that were
111 used for sample collection and desorption in the laboratory were from CTC Analytics (Zwingen,
112 Switzerland). An Agilent 6890N gas chromatograph coupled with an Agilent 5975C mass spectrometer
113 (Agilent Technologies, Pittsburg, PA, USA) was used for the method optimization and quality assurance tests
114 for air samples in the laboratory. For onsite analysis, an Agilent 6890 N gas chromatograph (Agilent
115 Technologies, Pittsburg, PA, USA) equipped with a lab made ITEX heater for thermal desorption was
116 employed and coupled to an Agilent 5973 mass spectrometer. The GC capillary column used for the
117 chromatographic separations was an InertCap™ for amines (30 m length x 0.25 mm i.d., without any
118 information for the film thickness, GL Sciences, Tokyo, Japan).

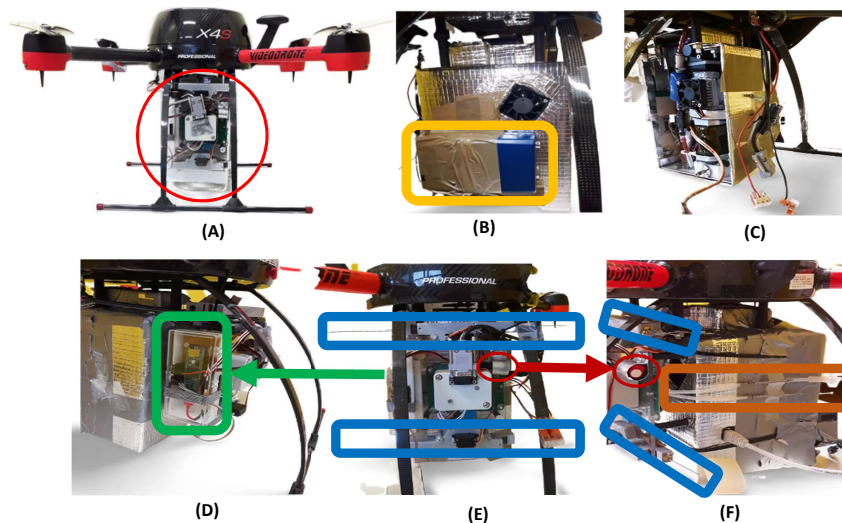


119 For organic acid determination, an Agilent 1260 Infinity high performance liquid chromatography (HPLC)
120 system equipped with a binary pump, autosampler, degassing unit, and a column compartment was employed
121 and coupled to an Agilent 6420 triple-quadrupole mass spectrometer with electrospray ion source (ESI)
122 (Agilent Technologies, Palo Alto, CA, USA). Chromatographic separations were performed with a 2.1x150
123 mm SeQuant[®]ZIC[®]-cHILIC (3 μm particle size) hydrophilic interaction liquid chromatography (HILIC)
124 column (MerckKGaA, Darmstadt, Germany). A KrudKatcher ULTRA HPLC in-line filter (0.5 μm) from
125 Phenomenex Inc (Torrance, CA, USA) protected the column from particulate impurities.

126 2.3. Drone platform construction

127 A remote-controlled Geodrone X4L (Videodrone, Finland), similar to that used in our previous studies (Lan
128 et al., 2021; Pusfitasari et al., 2022) with some modifications, was employed to carry out miniaturized air
129 sampling and analysis systems. With the dimension of 58x58x37 cm (width x depth x height), it could carry
130 the modified sampling box including our MAS system (up to four SPME Arrow units and up to four ITEXs)
131 with a new, light sampling pump for ITEX system. In addition, some portable devices were also attached to
132 the drone to measure Black Carbon (BC) and particle sizes by condensation particle counter (CPC). BC
133 portable device in the field was an AethLabs AE51-S6-1408, with the application version of 2.2.4.0 (San
134 Francisco, CA, USA). It operated at 880 nm wavelength, with the air flow-rate of 99 mL/min. The portable
135 CPC was a laboratory-made. The portable CPC measured total aerosol particle number concentration
136 between sizes from 20 nm and 5 μm . The references for BC and particle concentrations were measured at
137 Boreal forest SMEAR II Station at the altitude of 4 meters by an AE33 (operated at 880 nm) and an aerosol
138 electrometer (TSI 3772), respectively.

139



140

141 **Fig. 1.** Drone platform sampling system with: (A) Air sampling box carried by aerial drone. (B) BC placed
142 behind the box. (C) CPC inserted into the sampling box. (D) The right side of the sampling box is a sensor
143 that measured temperature and relative humidity. (E) Front position of the sampling box consisted of SPME
144 Arrow units (marked with blue) and a VOC sensor (red circle). (F) Sides of the sampling box included ITEX
145 unit and filter accessory (brown).

146 2.4. Gas chromatography-mass spectrometry analysis

147 The SPME Arrow and ITEX sampling systems were preconditioned at 250°C for 10 minutes under inert gas
148 N₂. Prior to sampling, decafluorobiphenyl vapor (as an internal standard) was spiked to SPME Arrow and
149 ITEX for 1 min and 5 mL, respectively. After sampling, the SPME Arrow unit was injected to the GC inlet
150 to desorb the analytes at the temperature of 250°C for 1 min. While for ITEX, 800 µL of He was aspirated to
151 the ITEX syringe and the analytes were desorbed at the temperature of 250°C and injected into the GC-MS
152 system by moving the plunger down with the injection speed of 200 µL s⁻¹. All the analyses were done in
153 splitless injection at 250°C. For chromatographic separations, the GC oven temperature was programmed
154 from 40 °C (held for 2 min) to 250 °C (held for 10 min) at a rate of 20 °C min⁻¹. The temperature of transfer
155 line, ion source and quadrupole were 250, 230 and 150 °C, respectively. Electron ionization (EI) mode (70
156 eV) was used, and the scan range was from m/z 15 to 350. Helium (99.996%, AGA, Espoo, Finland) was
157 used as a carrier gas at a constant flow rate of 1.2 mL min⁻¹.



158 **2.5. Hydrophilic Interaction liquid chromatography-tandem mass spectrometry method for organic**
159 **acids analysis**

160 Acetonitrile (ACN) was used as the main organic solvent containing 0.01% formic acid (FA) (as Eluent A),
161 while Eluent B is aqueous 0.01% FA solution. The applied LC gradient was the following: 5% B (0-6 min),
162 5 to 20% B (5-18 min), and post run for 15 min. The flow rate for the analysis was 0.25 mL/min and column
163 temperature was maintained at 40°C. The injection volume was 10 µl. The LC system was coupled to the
164 triple quadrupole mass spectrometer equipped with ESI. The ion source was operated in both positive and
165 negative modes.

166 **2.6. Method development, quality control and quality assurance studies.**

167 The optimization study for MCM-41-TP-ITEX system, including optimization of the adsorption and
168 desorption processes, sampling kinetics, breakthrough volume, and the recovery of the storage time, has been
169 carried out in our previous study using multivariate analysis (Pusfitasari et al., 2022). The evaluation and
170 validation of SPME Arrow units coated with MCM-41, DVB-PDMS, and carbon wide range (Carbon WR)
171 for the sampling of VOCs have also been studied in our previous research (Helin et al., 2015; Lan et al.,
172 2019b).

173 For TENAX-GR-ITEX sampler, the same method development and validation including the determination
174 of optimum flow rate, repeatability, reproducibility and sample storage were done by using our laboratory-
175 made autosampler. The repeatability and reproducibility of TENAX-GR-ITEX system were studied by
176 analyzing the model compounds with five different ITEX units five times, each. The sampling flow rate (47
177 mL/min) was measured at least once for each ITEX during the comparison.

178 The storage study was performed by keeping the TENAX-GR-ITEX system at room temperature and in a
179 freezer (-20 °C). The purpose was to monitor how conditions affect the adsorption of chemicals in
180 surrounding environment to TENAX-GR during storage. The retainment of adsorbed analytes in different
181 conditions was also monitored. The difference in recovery between control sample (not stored) and stored
182 sample was regarded as the loss of the compound.

183 **2.7. Application, measurement sites and sample collection in the field**

184 The field sampling was carried out at the SMEAR II Station (Station for Measuring Ecosystem–Atmosphere
185 Relations; (Hari and Kulmala, 2005), with the coordinate of 61.84263°N - 24.29013°E), Hyytiälä, from 4 to



186 14 October 2021. As many as 53 drone flights were performed and 135 air samples in total were collected
187 (67 samples were collected using ITEX and 68 using SPME Arrow sampling systems).

188 SPME Arrow units with different coating materials, DVB/PDMS, MCM-41, Carbon WR, were exploited to
189 collect gas phase samples. MCM-41-TP-ITEX and TENAX-GR-ITEX sampling systems were used to
190 simultaneously collect gas phase and particles. In the field study, the measured ITEX airflow ranged from 40
191 to 78 mL/min. The flow was carefully measured before the sampling and after analyte desorption. ITEX
192 sampling volumes were then obtained by multiplying the value of ITEX airflow rate with the sampling time.
193 Other sampling variables, such as sampling location, remained constant.

194 To study the average composition of VOCs in the atmosphere, the samples were collected simultaneously by
195 ITEX and SPME Arrow systems located on the drone at the altitudes from 50 m to 400 m. Composition
196 samples were collected for 2 min at each altitude and during the descending of the drone by starting at the
197 highest altitude of 400, followed by 300, 200, 100 and 50 m (Supplemental Figure S1). In this case, a total
198 sampling time was 13-14 minutes (consist of total of 10 min at different altitudes, and 3-4 minutes when the
199 drone was descending from 400 m to 50 m), with a total flight time close to 20 min including take-off and
200 landing.

201 The VOC composition at the altitudes of 50 m and 400 m was also separately determined. Detail schematic
202 picture on our sampling system is seen in the Supplemental Figure S2 (sampling at 50 m for 10 min) and
203 Supplemental Figure S3 (sampling at 400 m for 10 min).

204 Evaluation of ITEX sampling with filter accessory was also studied. TENAX-GR-ITEX furnished with filter
205 accessory was employed to collect the gas phase only. A polytetrafluoroethylene (PTFE) filter with the pore
206 size of 0.2 μm (diameter of 13 mm, VWR) was used as ITEX filter accessory to remove aerosol particles
207 from the natural air samples. The results obtained were directly compared with those achieved by Carbon
208 WR-SPME Arrow sampling system. Details about the experiments, sampling time and altitudes are found
209 from Supplemental Figure S1.

210 Suitability of particle trap for subsequent analysis was evaluated by the determination of the organic acids
211 retained or adsorbed in the filter accessory. Sample collection from drone at the altitude from 50 to 400 m is
212 seen in Supplemental Figure S4. Aerosol particles were collected onto the filter attached to ITEX unit in the
213 drone. All the collected samples were wrapped in aluminum foil and placed into separate Minigrip bags
214 which were stored in freezer ($-20\text{ }^{\circ}\text{C}$) prior to analysis.



215 Portable BC and CPC devices were always active on measuring BC and total particle numbers during the fly
216 of the drone. The detected BC and total particle numbers obtained with our portable devices were then
217 compared with those obtained with reference devices at the SMEAR II Station.

218 2.8. Data Processing and statistical analysis

219 Agilent ChemStation and Agilent Mass Hunter software were exploited for basic data processing, such as
220 peak identification and integration. An Mzmine2 (version 2.53) software, consisting of an algorithm
221 Automated Data Analysis Pipeline (ADAP-GC) was used for pre-processing untargeted mass spectrometric
222 data for detection, deconvolution, and alignment of the chromatographic peaks in natural samples (Lan et al.,
223 2021; Pusfitasari et al., 2022; Ruiz-Jimenez et al., 2019). NIST2020 (NIST MS Search v.2.3) mass spectral
224 database was used to check and compare the mass spectra of the aligned peaks as well as their retention
225 indices. The identified compounds should have a spectral match of >800 and ± 45 as the maximum difference
226 between experimental and library Kováts retention indices.

227 Partial least squares regression (PLSR) equations were developed for the quantification and semi-
228 quantification of the detected compounds in natural air samples (Kopperi et al., 2013; Lan et al., 2021;
229 Pusfitasari et al., 2022). To develop different PLSR equations for the quantification/semiquantification of
230 potentially identified compounds, six different concentration levels of 19 detected compounds, i.e. pyridine,
231 sec-butylamine, 1-butanamine, butanenitrile, 2-propen-1-amine, diethylamine, dimethylformamide,
232 hexylamine, trimethylamine, nonane, isobutanol, ethylacetate, methyl isobutyl ketone, hexanal, 2,3-
233 butanedione, benzaldehyde, acetophenone, p-cymene and ethyl benzene, were collected and analyzed under
234 optimal experimental conditions. Afterwards, the data was used for the development of the PLSR equation.

235 Total particle numbers measured by the reference instrument, an aerosol electrometer TSI 3772 at the altitude
236 of 4 meters (ground level), were downloaded directly from the SmartSMEAR open-access database:
237 <https://smear.avaa.csc.fi/> (Junninen et al., 2009).

238 The measured VOC values that were collected by ITEX sampling system, and BC as well as total particle
239 numbers at different altitudes were calculated to the same pressure level so that they could be compared to
240 literature values (Brasseur et al., 1999; Kivekäs et al., 2009; Rajesh and Ramachandran, 2018). In this study,
241 the reading values were corrected for ambient pressure and temperature as the following:

$$242 \quad A = m_A \left[\frac{P_0 T}{P T_0} \right]^{-1} \quad (1)$$



243 where A is the corrected value, m_a is the measured raw concentration, P_0 is the standard atmospheric pressure
244 (101.3 kPa), T_0 is the standard temperature (293 K), P is the ambient atmospheric pressure, and T is the
245 ambient temperature. Supplemental Table S1 shows the data at ambient temperatures and pressures used in
246 this study, as well as the calculated correction factors at different altitudes. In the case of VOC concentrations
247 collected by SPME Arrows, no correction was applied since the equilibrium constant for current adsorbents
248 and compounds was not studied at various pressures and temperatures.

249 3. Results and Discussion

250 3.1. Optimization of the sampling techniques using gas chromatography-mass spectrometry

251 The choice of coating materials for SPME Arrow sampling systems was based on the good selectivity of
252 MCM-41 for nitrogen-containing compounds, suitability of DVB/PDMS for most of the VOCs present in the
253 air samples, and the capability of Carbon WR to collect volatile compounds, covers a wide range of polarity
254 and have a good reproducibility (Kim et al., 2020; Lan et al., 2019b; Ruiz-Jimenez et al., 2019). Whereas for
255 ITEX sampling system, the MCM-41-TP was chosen as a sorbent material since it has proved to have good
256 selectivity towards nitrogen-containing compounds, while TENAX-GR was selected due to its good
257 capability to collect different VOCs present in the air (Lan et al., 2019a; Pusfitasari et al., 2022).

258 The optimization containing equilibrium sampling time for SPME Arrow sampling systems, breakthrough
259 volume for MCM-41-TP-ITEX, desorption temperature and desorption time towards representative
260 compounds such as diethylamine, trimethylamine, isobutylamine, pyridine, p-cymene, hexanal, and
261 acetophenone have been tested in our previous studies. Briefly, the average sampling time that is used before
262 reaching equilibrium for both MCM-41-Arrow and DVB/PDMS-Arrow units is about 20 minutes. The
263 cleaning and desorption temperature of 250°C for 10 min and 1 min, respectively, were selected to be optimal
264 for the conditioning and analysis. The Carbon WR-Arrow sampling system was also treated in the same way
265 in terms of conditioning and desorption methods.

266 In our previous study, TENAX GR as the sorbent for ITEX's trap-accessory was able to adsorb mostly non-
267 nitrogen containing compounds and only a small amount of nitrogen containing compounds (Pusfitasari et
268 al., 2022). In the present study, universal TENAX-GR was used as ITEX sorbent material to collect air
269 samples. Desorption and conditioning processes were optimized using a previously developed methodology
270 and optimal conditions similar to MCM-41-TP-ITEX system with selective sorbent (section 2.4). The
271 repeatability of TENAX-GR-ITEX sampler was also tested, with the RSD between 3.4 and 7.1%



272 (Supplemental Tables S2 and S3), whereas the reproducibility between different ITEX units caused also by
273 ITEX manual packing was between 4 and 18%.

274 The sampling systems used in this study needed to be stored for a certain period of time before analysis to
275 accommodate the on-field situation. In our previous study, the sorbent in MCM-41-TP ITEX system could
276 be stored at -20°C up to 18 hours without losing much of the model compounds, with the recoveries of around
277 80 % (Pusfitasari et al, 2021). For TENAX-GR sorbent, the recoveries of 98% were obtained after storage
278 at -20°C for 24 hours, but only 78% when the sorbent was stored at room temperature for 24 hours. In this
279 study, the samples collected at the SMEAR II Station had to be analysed after storage of around 2 hours since
280 the samplers were needed for the upcoming field measurements. Therefore, both MCM-41-TP- and TENAX-
281 GR-ITEX systems were stored at room temperature only for a few hours before the analysis.

282 3.2. Optimization of organic acid analysis using hydrophilic interaction liquid chromatography 283 (HILIC)- tandem mass-spectrometry

284 HILIC-ESI-MS/MS was employed for analysis of organic acid from filter samples. 18 different acids were
285 successfully identified and five of them were quantified using the optimized method. For the 18 model acids,
286 HILIC mobile phase with composition of ACN 80 % (solvent A) and 20% of 0.005% FA (solvent B) was
287 chosen as the best eluent for acids separation (Supplemental Table S4). The second optimized parameter was
288 drying gas temperature which is important parameter in the ESI technique to allow the eluent from the HILIC
289 column to evaporate as rapidly as possible in the ion source (Kruve, 2016). In this study, using the selected
290 optimum eluent, i.e. ACN (80 %) and 0.005% FA (20%), with the flow rate of 0.25 mL/min, the drying gas
291 temperature of 275°C was selected as the optimum temperature. Supplemental Table S5 shows the established
292 multiple reaction monitoring (MRM) method parameters for each compound using all optimized parameters
293 including the optimized voltages for other crucial parameters, namely fragmentor voltage, collision energy
294 and cell acceleration voltage (CAV).

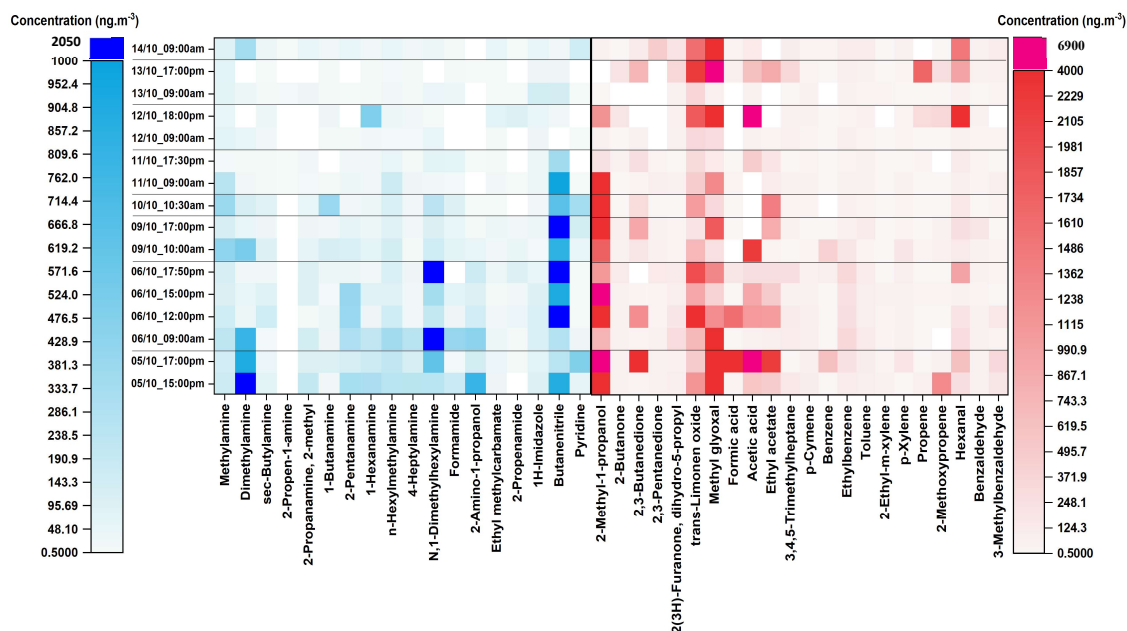
295 3.3. Application of air sampling system at the altitude from 50 to 400 m

296 In this study, the mesoporous silica-based materials, namely MCM-41 and MCM-41-TP, were used to
297 selectively collect nitrogen-containing compounds (Lan et al., 2019b; Pusfitasari et al., 2022). Whereas the
298 commercial universal materials, TENAX-GR and DVB/PDMS were also used to collect other than nitrogen-
299 containing compounds.



300 MCM-41-TP-ITEX and TENAX-GR-ITEX sampling systems were used to collect atmospheric air samples
301 containing both gas phase and aerosol particles, while the samples containing only gas-phase were collected
302 by MCM-41-SPME Arrow and DVB/PDMS-Arrow systems. The concentrations in aerosol particles were
303 obtained via the subtraction of these results, i.e. MCM-41-TP-ITEX subtracted with MCM-41-SPME Arrow,
304 and TENAX-GR-ITEX subtracted with the DVB/PDMS-SPME Arrow.

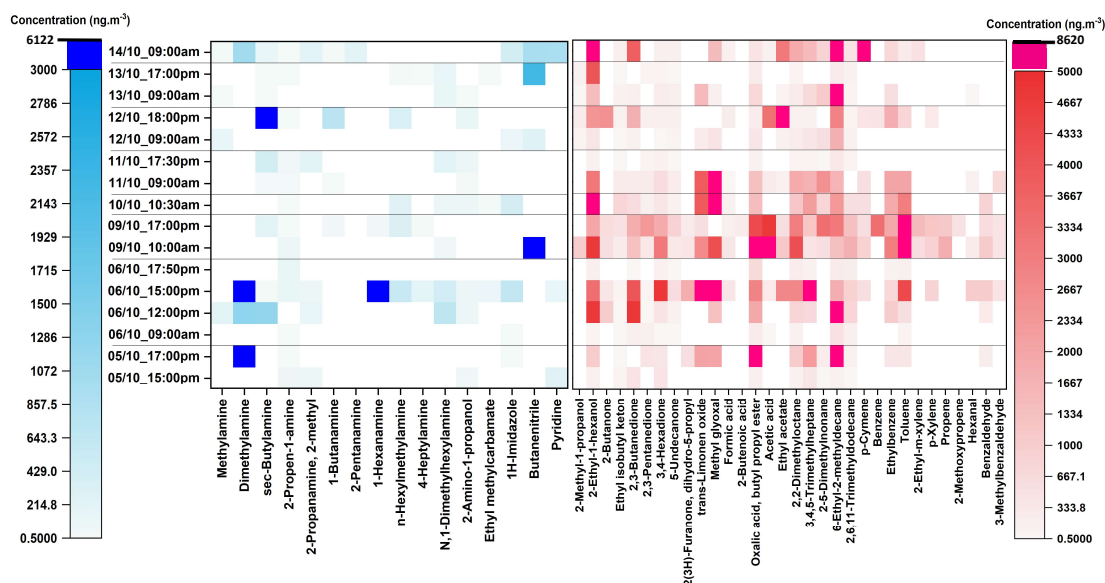
305 Altogether, up to 40 VOCs were detected in gas phase and 48 were in particle phase samples. VOCs with
306 various functional groups such as nitrogen-containing compounds, alcohols, ketones, aldehydes, small
307 organic acids, and hydrocarbons were detected both by selective MCM-41 coated SPME Arrow and MCM-
308 41-TP-ITEX sampling systems and by universal sorbent materials TENAX-GR-ITEX and DVB/PDMS
309 coated Arrow systems. However, because in our previous study (Lan et al., 2019b; Pusfitasari et al., 2022),
310 the MCM-41-SPME Arrow and MCM-41-TP-ITEX samplers gave sensitive and reliable results in collecting
311 selectively nitrogen-compounds, only the results obtained by MCM-41-Arrow and MCM-41-TP-ITEX
312 samplers are shown for nitrogen-containing compounds in this section. While data for other VOCs were
313 collected using ITEX with universal sorbent materials TENAX-GR and using DVB/PDMS coated SPME
314 Arrow.



315



316 **Fig 2.** Concentrations of nitrogen-containing compounds (left) and other VOCs (right) in the gas-phase at the
317 SMEAR II Station, Hyytiälä at the mixed altitude between 50 and 400 m. Nitrogen-containing compounds
318 (left) were collected using MCM-41-SPME Arrow system with selective sorbent, while other VOCs (right)
319 were collected using DVB/PDMS-SPME Arrow system with universal sorbent. White color = not detected.
320



321

322 **Fig 3.** Concentrations of nitrogen-containing compounds (left) and other VOCs (right) in the particle phase
323 at SMEAR II Station, Hyytiälä at the mixed altitude between 50 and 400 m. Samples were collected using
324 MCM-41-TP-ITEX system with selective sorbent (left) and TENAX-GR-ITEX systems with universal
325 sorbent (right). White color = not detected.

326 As can be seen from Figure 2, eleven aliphatic amines (methylamine, dimethylamine, sec-butylamine; 2-
327 propen-1-amine; 2-methyl-2propanamine; 1-butanamine, 2-pentanamine, 1-hexanamine, n-
328 hexylmethylamine, 4-heptylamine, N,1-dimethylhexylamine) and seven other nitrogen-containing
329 compounds (formamide, 2-amino-1-propanol, ethylmethylcarbamate, 2-propenamide, 1H-imidazole,
330 butanenitrile, and pyridine) were detected, quantified and semi quantified in gas phase samples with the
331 concentrations up to 2005 ng m⁻³. While in the particle phase (Figure 3), the total of 16 nitrogen-containing
332 compounds was detected with the concentrations up to 6122 ng m⁻³. These results are comparable to our



333 previous study in which the concentrations of nitrogen-containing compounds were up to 2930 ng m⁻³ and
334 5480 ng m⁻³ in gas phase and particle phase, respectively (Pusfitasari et al., 2022). However, the samples
335 were collected then at the altitude from 50 to 150 m (Pusfitasari et al., 2022).

336 Dimethylamine, that can be produced by animal husbandry, cattle, landfill, sewage, and also industry (Ge et
337 al., 2011), was detected in both gas and particle phase during afternoon with the concentrations up to 1004
338 ng m⁻³ for gas phase, and up to 5909 ng m⁻³ for the particle phase (Figure 2-left and Figure 3-left). Studies
339 have indicated that organic amines, including DMA, can be present to large extent in the particles e.g. by
340 transferring from gas phase to particles (Chen et al., 2022; Yu et al., 2017; Zhao et al., 2007). DMA is one
341 of the most common and abundant amines found in the atmosphere, and particulate DMA concentrations can
342 increase due to enhanced BVOC emissions and due to aerosol-phase water that increase their partition to the
343 condensed phases (Chen et al., 2017; Ge et al., 2011; Youn et al., 2015).

344 Other amines that were detected at high concentrations were methylamine, pentanamine, hexanamine,
345 hexylmethylamine, and dimethylhexylamine with the concentrations up to 432, 395, 493, 340, and 1393 ng
346 m⁻³, respectively (Figure 2-left). For the particles, sec-butylamine was detected with the concentrations up to
347 4090 ng m⁻³, hexanamine up to 4316 ng m⁻³ and dimethylhexylamine up to 686 ng m⁻³ (Figure 3-left).

348 For nitrogen-containing compounds other than amine, butanenitrile was detected as the highest
349 concentrations up to 2005 ng m⁻³ in gas and 6122 ng m⁻³ in particle phases. 2-Amino-1-propanol, pyridine,
350 and 1-H-imidazole were present in gas phase as the second, third and fourth highest concentrations up to 790,
351 492, and 136 ng m⁻³, respectively. While in the particle phase, their concentrations were up to 129, 958, and
352 646 ng m⁻³, respectively. The concentrations of all detected nitrogen-containing compounds at mixed
353 altitudes can be seen in Supplemental Table S7.

354 For other VOCs, 22 compounds in gas phase (Figure 2-right) and 32 in particle phase (Figure 3-right),
355 containing alcohols, aldehydes, ketones, small organic acids and hydrocarbons were detected and quantified
356 or semi quantified with the concentrations up to 6898 ng m⁻³ in the gas phase and 8613 ng m⁻³ in the particle
357 phase. In the gas phase, 2-methyl-1-propanol; 2,3-butanedione; trans-limonene oxide, methylglyoxal, acetic
358 acid, ethyl acetate, and hexanal were discovered almost all the time during the samplings with the
359 concentration up to 4209, 2436, 2210, 4695, 6898, 2198 and 3984 ng m⁻³, respectively (Figure 2-right). While
360 in the particle phase, almost all detected compounds were present in high concentrations such as 2-ethyl-1-
361 hexanol (4114 ng m⁻³); 2,3-butanedione (4865 ng m⁻³), trans-limonene oxide (6886 ng m⁻³), methylglyoxal
362 (8613 ng m⁻³), aliphatic hydrocarbons (7091 ng m⁻³), ethyl benzene (3042 ng m⁻³) and toluene (7715 ng m⁻³)



363 , (Figure 3-right). Supplemental Table S8 gives at mixed altitudes (50 to 400 m) the concentrations for all
364 detected VOCs that do not belong to nitrogen-containing compounds.

365 In the atmosphere, 2,3-Butanedione is naturally occurring in food products such as butter and beers (Boylstein
366 et al., 2006), while trans-limonene oxide is detected possibly due to the partial oxidation of monoterpene
367 limonene's olefinic bonds (Hoeben et al., 2012; Karlberg et al., 1992). Methylglyoxal, an important precursor
368 of SOA, is produced in the atmosphere by the oxidation of hydrocarbons, such as isoprene, acetylene, toluene,
369 and xylenes (Fu et al., 2013; Olsen et al., 2007; Zhang et al., 2016). Other detected compounds, e.g. acetic
370 acid and ethyl acetate can be released from different sources such as biomass burning and vegetation (Khare
371 et al., 1999; Rosado-Reyes and Francisco, 2006).

372 The diurnal pattern in both gas and particle-phases was also observed. As can be seen from Figure 2 in the
373 gas phase, aliphatic amines that are mostly emitted by biogenic sources were present in lower concentrations
374 in the evening (started at 17:00 pm) compared to daytime, whereas some amines, namely hexanamine and
375 dimethylhexylamine, had slightly higher concentrations in the evening. These results agree well with our
376 previous study in which most of the amines had a diurnal variation with a daytime maximum due to their
377 dependency on temperature for their emission, indicating the contribution to biogenic sources (Pusfitasari et
378 al., 2022). High concentrations of some amines in the evenings could be caused by the weak atmospheric
379 mixing at night resulting in decreased reactions with atmospheric acids (Hemmilä et al., 2018). In contrast,
380 VOCs that were emitted from other sources had higher concentrations mostly in the afternoons, except for
381 non-nitrogenated compounds with high concentrations also in the mornings on 11 October 2021. The
382 anthropogenic sources that might affect this result, were probably carried by the wind from other places and
383 were mixed in the atmosphere since the samples were collected at high altitudes (up to 400 m). In the particle
384 phase, there was no clear pattern seen since our samples were mostly collected only in the mornings and late
385 afternoons. However, in our previous study we found that VOCs had high concentrations in mornings and
386 evenings since temperature dependency affects the deposition of amines in the colder evenings, and then they
387 partition back to the atmosphere in the higher temperature mornings (Pusfitasari et al., 2022). In this present
388 study we can also see from Figure 3 high concentrations both in the mornings and late afternoons, but
389 surprisingly also at noon (on 6 October).

390 The correlation among all the VOCs in both gas and particle phases was also studied. R-value close to one
391 and P-value <0.05 mean that there is correlation between variables. As can be seen from Supplemental Figure
392 S5, only a few compounds in gas phase correlate with those detected in the particle phase, such as particulate



393 benzaldehyde that correlated with alcohol vapors (i.e. gas-phase of 2-methyl-1-propanol and 2-ethyl-1-
394 hexanol) and some amines (i.e. methylamine, sec-butylamine, 2-pentanamine, and n-hexylmethylamine).
395 These correlations can be explained by the studies conducted by Perez et al (2017) who was investigating the
396 implication of aldehyde – amines to the aerosol growth by providing low-energy neutral pathways for the
397 formation of larger and less volatile compounds (Perez et al., 2017).

398 In addition, we can also see that some nitrogen-containing compounds correlated with aliphatic
399 hydrocarbons, aliphatic carbonyl, and aliphatic alcohols in the gas phase, indicating that they might be
400 emitted from the same sources. This finding is supported by the study conducted by Isidorov *et al* (2021).
401 Although their group could not detect selectively nitrogen-containing compounds because they used
402 universal sorbent material for the collection of air sample (i.e. DVB/CAR/PDMS-SPME), they could detect
403 all other VOCs compounds at the same time from the boreal forest (Isidorov et al., 2022).

404 **3.4. Evaluation of ITEX filter accessories**

405 In our previous study, it was proved that a small filter can be used to trap particles allowing only gas phase
406 enter the ITEX sampler (Pusfitasari et al., 2022; Ruiz-Jimenez et al., 2019). The experiments were properly
407 designed to check and compare the results achieved for gas phase compounds using a passive SPME Arrow
408 and an active ITEX + filter sampling systems. In the present study, the samples were collected from 11 to 14
409 October 2021 and TENAX-GR-ITEX was exploited with the filter accessory. The altitudes for these
410 experiments were 50-400 m (Supplemental Figure S1). As can be seen in Supplemental Figure S6, aliphatic
411 amines were the major nitrogen-containing compounds detected both in the gas and particle phases. For
412 VOCs without any nitrogen compounds, following the results in the previous section (i.e. section 3.3.),
413 alcohols, ketones, aldehydes, organic acids and some hydrocarbons were detected, quantified and
414 semiquantified with the concentrations shown in Supplemental Figure S6. The results of the gas-phase
415 sampled by ITEX system with filter accessory were comparable with the gas phase results obtained by the
416 SMPE Arrow sampling system.

417 In addition to the comparison of gas phase collected by ITEX (+ filter accessory) and SPME Arrow systems,
418 the recoveries of gas phase obtained by the first sampling system were also evaluated. The recoveries of non-
419 polar compounds, such as alkanes, were only <50% (Supplemental Table S9). The more polar compounds,
420 such as alcohols, acids, and nitrogen-containing compounds, were mostly detected at higher recoveries from
421 50% up to 99%. Most probably non-polar compounds of the gas phase were partly adsorbed to the ITEX
422 filter accessory that was made from PTFE (Parshintsev et al., 2011). PTFE has a non-polar structure due to



423 the distribution of the fluorine atom around the carbon polymer backbone which balances the electronegative
424 and electropositive charges (Parsons et al., 1992). Hence, our study proved that ITEX with PTFE filter does
425 not only trap aerosol particles but is also excellent for the collection of polar compounds, such as nitrogen-
426 containing compounds, of gas phase. Nevertheless, since nitrogen-containing compounds are very water
427 soluble, the humidity level in the air will most likely affect the distribution of polar compounds between the
428 filter and ITEX adsorbent, e.g. water condensing to the filter at high humidity.

429 3.5. Analysis of aerosol particles collected by ITEX with PTFE filter using liquid chromatography 430 tandem mass spectrometry

431 Filter collecting aerosol particles in ITEX was extracted and analyzed separately by using HILIC-MS/MS to
432 quantify carboxylic and dicarboxylic acids since most organic acids cannot be analyzed by GC without
433 derivatization, except small organic acids such as formic acid and acetic acid. The organic acids have
434 capability to significantly enhance the hygroscopicity of aerosol particles and contribute to the acidity of
435 precipitation and cloud water.

436 As can be seen in Table 1, five main acids, succinic acid, benzoic acid, phthalic acid, glutaric acid, and adipic
437 acid, were identified and quantified. Succinic acid was observed almost in every sample and its higher
438 prevalence could possibly be explained by the fact that it can be formed from common biogenic and
439 anthropogenic precursors such as isoprene and toluene (Sato et al., 2021). The aromatic acids such as benzoic
440 acid and phthalic acid were also detected in the samples. The concentrations of benzoic acid (up to $1.4 \mu\text{g}/\text{m}^3$)
441 were higher than those of phthalic acid (up to $0.77 \mu\text{g}/\text{m}^3$). Observation of these acids is relevant as their
442 aromatic hydrocarbon precursors are common in the atmosphere. In addition, phthalic acid has also been
443 detected in the summer 2012 samples, but then no benzoic acid was detected in the gas phase or particulate
444 phase (Kristensen et al., 2016).

445 **Table 1.** Concentrations of acids collected from the ITEX filters at the altitudes of 50-400 m.

Sampling time	Succinic acid (ng/m ³)	Benzoic acid (ng/m ³)	Phthalic acid (ng/m ³)	Glutaric acid (ng/m ³)	Adipic acid (ng/m ³)
	HA	HA	HA	HA	HA
11.10.2021	1416	1416	657	1619	10926
12.10.2021	435-789	1416	769	n.d.	n.d.
13.10.2021	496-4654	n.d.	n.d.	n.d.	n.d.
14.10.2021	n.d.	n.d.	n.d.	1720	6374

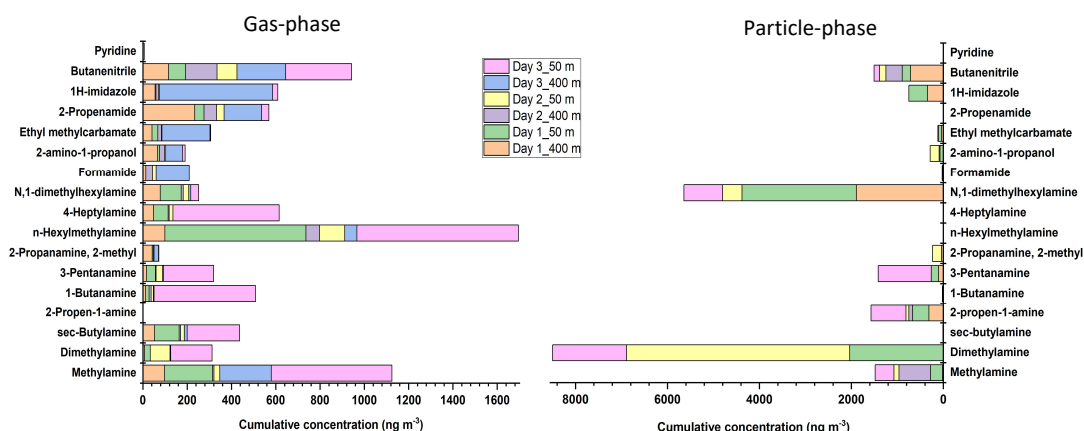
446 *n.d. = not detected



447 Glutaric and adipic acids were also determined from samples taken on the 11th and 14th of October. Glutaric
448 acid and adipic acid have been commonly detected in atmospheric aerosols and cloud droplets (Wen et al.,
449 2021). Other dicarboxylic acids, such as glycolic acid and cis-pinonic acid were detected in only one sample
450 in which their LODs were exceeded (Supplemental Table S10). The possible reason for the low concentration
451 of glycolic acid might be that it can be formed as an oxidation product of biogenic isoprene (Liu et al., 2012).

452 3.6. Comparison of nitrogen-containing compounds and other VOCs at the altitudes of 50 m and 400 453 m

454 The aim of this study was to compare the composition of VOCs at the altitudes of 50 m and 400 m, separately.
455 Carbon WR-SPME Arrow unit with universal sorbent was used to collect a wide range of VOCs in the gas
456 phase. MCM-41-TP-ITEX and TENAX-GR-ITEX sampling systems were employed to collect gas and
457 particle phases.



458

459 **Fig. 4.** Concentrations of nitrogen-containing compounds in the gas-phase (left) and in particle-phase (right)
460 at SMEAR II Station at altitudes 50 and 400 m for three days (8 to 10 October 2021). For the gas-phase
461 samples were collected using Carbon WR-Arrow sampling system (left), and the particle-phase samples were
462 collected by MCM-41-TP-ITEX system (right). The concentrations of aerosol particle compounds were
463 obtained via subtraction the results obtained by MCM-41-TP-ITEX from those obtained by Carbon WR-
464 Arrow with universal sorbent.

465 As can be seen from Figure 4, the concentrations of amines that were emitted by biogenic sources, such as
466 methylamine, dimethylamine, sec-butylamine, butanamine, pentanamine, hexylmethylamine, and

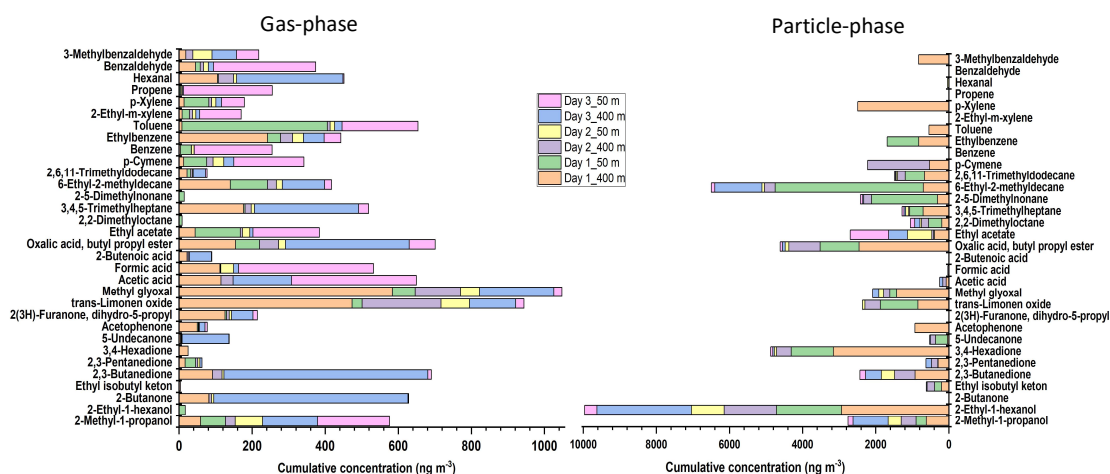


467 heptylamine, were mostly found at higher concentrations at the lower altitude (50 m). The concentrations
468 were decreased at higher altitude 400 m most probably due to the dilution (since the sources are on the
469 ground) and reaction with hydroxyl radical (Kieloaho, 2017).

470 For nitrogen containing compounds, other than amines, imidazole was one of the compounds detected by our
471 system. There have been a number of laboratory studies where imidazole has been reported to be the major
472 product of glyoxal reaction with ammonium ions or primary amines on secondary organic aerosol. In
473 addition, imidazoles can become a secondary product of the reaction of dicarbonyls with nitrogen containing
474 compounds, therefore they might have potential to act as photosensitizers triggering secondary organic
475 aerosol growth and are forming constituents of light absorbing brown carbon (De Haan et al., 2011; Dou et
476 al., 2015; Teich et al., 2020). Imidazoles were detected mostly in the particle phase with concentrations up
477 to 422 ng m^{-3} at 50 m and 338 ng m^{-3} at 400 m. Slightly lower concentrations were discovered in the gas
478 phase with the values up to 58 ng m^{-3} at the altitudes of 50 m, and 510 ng m^{-3} at the altitude of 400 m.

479 Other nitrogen-containing gas phase compounds detected, such as formamide, 2-amino-1-propanol,
480 ethylmethylcarbamate, and propenamide showed also the same pattern with higher concentrations at 400 m
481 than at 50 m. These compounds were most probably transported by the wind from other areas and emitted by
482 various sources, such as biomass burning, peatland, industries, and other anthropogenic sources (Pusfitasari
483 et al., 2022).

484



485



486 **Fig. 5.** Concentrations of non-nitrogenated VOC compounds in the gas-phase (left) and in particle-phase
487 (right) at SMEAR II Station at altitudes 50 and 400 m for three days (8 to 10 October 2022). The gas-phase
488 samples were collected using Carbon WR-Arrow system (left), and particle-phase samples using TENAX-
489 GR-ITEX sampling systems (right). The concentrations of aerosol particle compounds were obtained via
490 subtraction the results obtained by TENAX-GR-ITEX from those obtained by Carbon WR-Arrow with
491 universal sorbent.

492 As can be seen from Figure 5 gas-phase VOC compounds without nitrogen (left side), such as trans-limonene
493 oxide, methylglyoxal, hexanal and ketones have higher concentrations at the altitude of 400 m compared to
494 50 m. Whereas some acids, such as acetic acid and formic acid, ethyl acetate, and BTX (benzene, toluene,
495 xylene) were mostly discovered at the altitude of 50 m. In the case of alcohols, they had comparable
496 concentrations at both 50 and 400 m. In the particle phase, most of the compounds had higher concentrations
497 at 400 m than at 50 m, except for some hydrocarbons (such as 2,5-dimethylnonane and 6-ethyl-2-
498 methyldecane) that had high concentrations at 50 m.

499 Alcohols are a prevalent class of VOCs in the atmosphere and can be emitted by biogenic sources such as
500 rain forest, and also from anthropogenic sources such as alcohol-gasoline blended fuel and industries
501 (McGillen et al., 2017; Nguyen et al., 2001). Therefore, it is no wonder that in this study alcohol was found
502 almost in all altitudes. The alcohol emission is becoming concern since it can react with Criegee intermediates
503 (product of biogenic alkenes oxidized by ozone) to produce α -alkoxyalkyl hydroperoxides (AAAHs) that can
504 lead to the formation of secondary organic aerosols (Bonn et al., 2004; McGillen et al., 2017; Sahli, 1992).

505 In the gas phase samples, benzene, toluene, and p-xylene (BTX) were found mostly at the altitude of 50 m
506 with the concentrations up to 219, 410, and 70 ng m^{-3} , respectively. Since BTX can be emitted from the
507 gasoline (major fuel of vehicles) and the samples were collected close to the parking area, the higher
508 concentrations were found at lower altitude 50 m. This finding is comparable with the study conducted by
509 Chen et al (2018) who measured the BTX concentrations between 100 and 300 ng m^{-3} from forest canopy at
510 the altitude between 20 and 26 m^{-3} (Chen et al., 2018; Yassaa et al., 2006). Toluene and p-xylene were also
511 detected in the particle phase as VOCs may be adsorbed onto the surface of the particles (Dehghani et al.,
512 2018; Kamens et al., 2011). The higher concentrations were detected at the altitude of 400 m with the
513 concentrations of up to 539 ng m^{-3} and 2475 ng m^{-3} for toluene and p-xylene, respectively. BTX play an
514 important role in the atmosphere since they have been recognized as important photochemical precursors for
515 the secondary organic aerosol (Correa et al., 2012; Ng et al., 2007).



516 Aldehydes in the atmosphere are also of concern because of their heterogeneous reaction with acids affecting
517 the particle growth (Altshuller, 1993; Jang and Kamens, 2001). In our study, some aldehydes, such as
518 methylglyoxal, hexanal and benzaldehyde, were found both in the gas and particle phase at the altitude of
519 400 m in higher concentrations than at the altitude of 50 m. At the altitude of 400 m, methylglyoxal was the
520 most abundant aldehyde with the concentrations up to 580 ng m^{-3} in the gas phase, and 1418 ng m^{-3} in the
521 particle phase. Ketones in aerosol particles have been associated with burning and non-burning forest, and it
522 represented up to 27% of the current organic aerosol mass concentration (OM) (Takahama et al., 2011).
523 Ketones were also found in this study at higher concentrations at high altitude 400 m in both gas phase and
524 particle phase.

525 The last group of chemicals that was detected by our collection systems was small organic acids, and from
526 these especially formic acid and acetic acid. Organic acids have an important role as chemical constituent in
527 troposphere and they contribute with a large fraction (25%) to the nonmethane hydrocarbons in the
528 atmosphere. The organic acids contribute to the acidity of precipitation and cloud water (Khare et al., 1999).
529 Acetic acid was found in both gas and particle phases at the altitudes of 50 and 400 m. However, the amount
530 of both formic acid and acetic acid found in the gas phase was higher than that in the particle phase. These
531 acids can originate from various sources such as vehicular emissions, ants, plants, soil, and biomass burning
532 (Zhang et al., 2022).

533 **3.7. Evaluation of total particle numbers and black carbon at high altitudes. Portable CPC and BC** 534 **devices carried by aerial drone**

535 The particle number concentration and BC concentration were measured by using portable CPC and BC
536 measurement devices carried by the drone. The BC concentration was measured at 880 nm wavelength (near
537 IR), as at this wavelength BC has strong absorption and least interferences by other organic molecules
538 (Dumka et al., 2010). The results were compared to those measured by the reference instruments at the
539 SMEAR II Station. The correction factors to the same pressure level as described in section 2.8 were
540 calculated with the values between 0.994 and 1.035 (Supplemental Table S1). Supplemental Figure S7 for
541 CPC proves a correlation between the results obtained by our portable CPC and reference instrument, with
542 direct linear close to 1 (R^2 of 0.9564). Oppositely, linear correlation for BC was only 0.2492, indicating that
543 there was no correlation between the reference instruments and our BC meter in the drone.

544 Our portable BC monitor in the drone gave higher concentration values than the reference one, located at 4m.
545 The reasons for the differences could be caused by amplification factor that raised due to multiple scattering



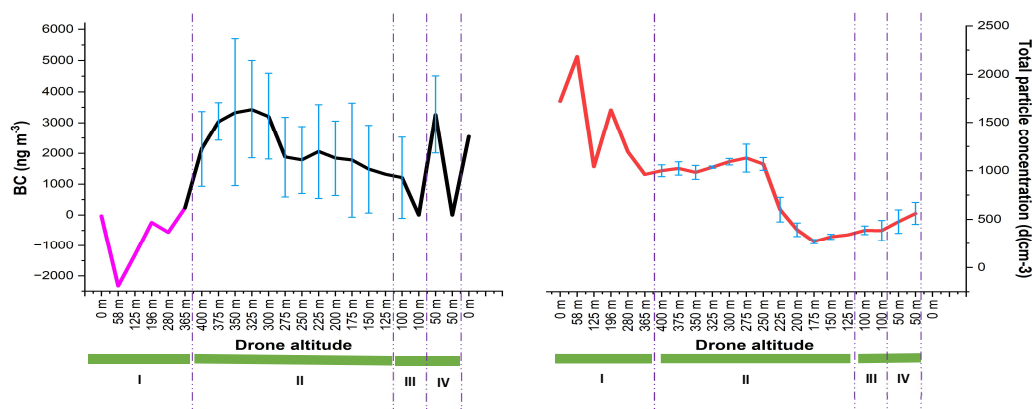
546 in quartz fiber matrix of the tape of the Aethalometer. The deposition of scattering material along with BC
547 to the filter tape produced the “shadowing effect” causing the BC meter to show higher concentration values
548 (Dumka et al., 2010; Weingartner et al., 2003). Alternatively, the differences can be explained by different
549 measurement altitudes between the reference instrument (measured at 4 m) and BC monitor in the drone (up
550 to 400 m). At lower altitude, living activities such as heating sauna and fuel burning from cars nearby the
551 area might contribute to the results, while at higher altitudes BC long distance transport contributes to the
552 results as well (Meena et al., 2021). The atmospheric boundary layer height (ABLH) also plays an important
553 role to govern concentration of BC at high altitudes since it can affect pollutant aggregation, transmission,
554 wet deposition, and dry sedimentation (Meena et al., 2021). The boundary layer (BL) is the lowest part of
555 troposphere and connects the ground and the free atmosphere. The average boundary layer height at Hyytiälä
556 SMEAR II Station in autumn (October) was around 500 m (Sinclair et al., 2022), explaining why we found
557 higher BC concentration at high altitudes. For comparison, Table 2 shows the BC mass concentrations
558 measured at high altitudes in different areas.

559 Table 2. Average BC concentrations observed at different locations.

Location	Altitude	Environment	Average BC concentration (ng m ⁻³)	Reference
Hyytiälä, Finland	100 m	Rural	2278±1188	This study
Hyytiälä, Finland	200 m	Rural	2500±1497	This study
Hyytiälä, Finland	300 m	Rural	3564±1648	This study
Hyytiälä, Finland	400 m	Rural	3909±729	This study
Mahabaleswar, India	1378 m	Rural	2600 ± 260	(Meena et al., 2021)
Mountain Huang, China	1840 m	Rural	1663±919	(Pan et al., 2011)
Port Blair, India	73 m	Rural	2446±66	(Moorthy and Babu, 2006)
Sinhagad, India	1300 m	Rural	1500	(Safai et al., 2007)

560

561 Autumn average of BC pollution in Hyytiälä according to Hyvärinen *et al.* 2011 was about 1291 ng m⁻³,
562 while Hienola *et al.* (2013) reported the October average was 550 ng m⁻³ (Hienola et al., 2013; Hyvärinen et
563 al., 2011). However, those studies were conducted using reference instrument at low altitude, i.e. 4 meters
564 above the ground.



565

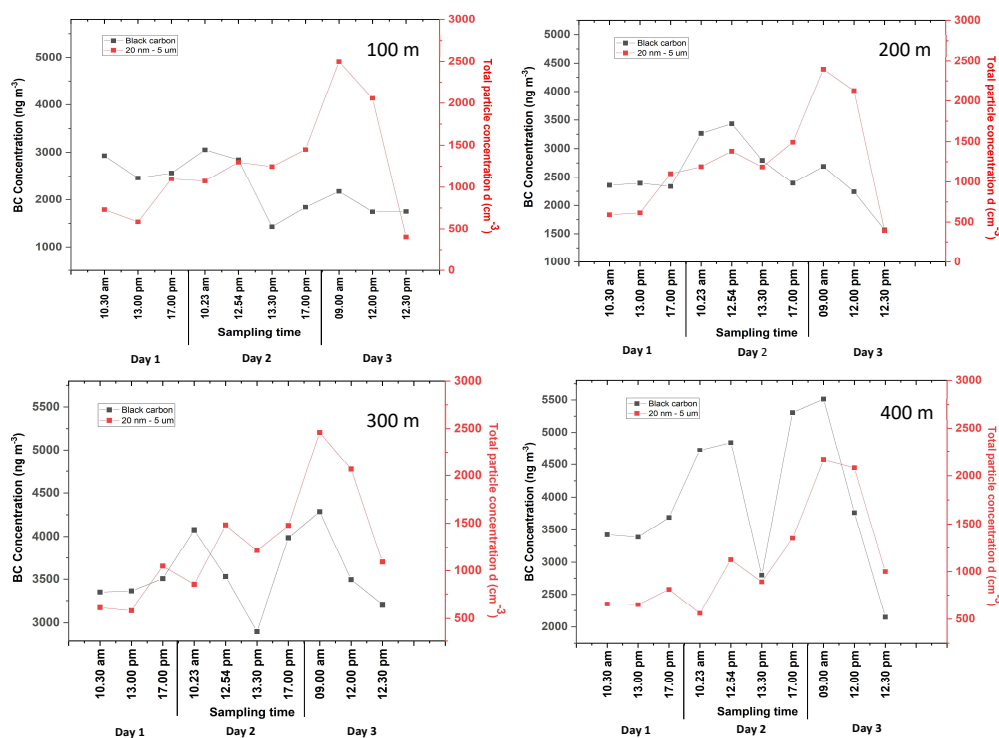
566 **Fig 6.** Evaluation of drone's vertical and horizontal movements. I = Drone is moving up with the speed of
567 2.5 ms^{-1} . II= Drone is descending with the speed of 1.25 ms^{-1} to each altitude before staying for 30 s. III and
568 IV = Horizontal movement to 100 m far with the speed of 5 ms^{-1} .

569 The drone stability was evaluated during the vertical and horizontal movements (drone movement schematic
570 is showed in Supplemental Figure S4). Figure 6 shows that the BC concentration and total particle numbers
571 were affected by the drone movements. Rapid ascending (area number I) affected both BC and CPC. BC
572 measurements showed negative values when the drone started warming up, take off, and then quickly moved
573 vertically with the speed of 2.5 ms^{-1} . These readings could be due to the temperature change on the BC sensor
574 when the drone ready to take off and drone fast ascending (Elomaa, 2022; Pan et al., 2011). Portable CPC
575 device gave also fluctuating data. Both BC device and CPC started to stabilize when approaching altitude of
576 365 m.

577 At the beginning of drone vertical movement at the altitude of 400 m, portable CPC gave more stable results
578 when the speed was decreased and when it was allowed to stabilize for 30 seconds (as can be seen in area
579 number II), resulting in smooth changes in the total particle numbers and some deviations at each altitude.
580 However, BC concentration varied also with high standard deviations at high altitude without any specific
581 movement, indicating that the drone movement influenced the portable BC device. Pan *et al* (2011) have
582 suggested that a large variation in the BC measurements could be caused by several factors such as boundary
583 layer stratification and turbulence. In addition, BC sensor was also very sensitive to change in temperature.
584 They observed that BC concentration could change quickly only after a short period of sunshine. Based on



585 the standard deviations' horizontal movements (area numbers III and IV), affected much less portable CPC,
586 compared to the portable BC.



587

588 **Fig 7.** Time series evaluation of CPC and black carbon at the heights of 100, 200, 300, and 400 m. Sampling
589 was conducted on October 9 (Day 1), 10 (Day 2), and 11 (Day 3), 2021. The values and point averages are
590 shown in Supplemental Table S11.

591 It can be seen from the results of Figure 7 for three days measurements that BC and CPC had similar pattern
592 at all altitudes (100, 200, 300 and 400 m). The daily means of total particle numbers are found from
593 Supplemental Table S12. Although the concentrations at the altitude of 400 m seem to be slightly lower than
594 those detected at lower altitudes, the patterns of total particle number are similar at every altitude (Figure 7),
595 most possible due to the limited anthropogenic activities near the sampling site. The potential mixing and the
596 particle formation in the atmosphere most likely influenced the total particle number detected. In addition,



597 particulates' long-range transport from different areas could also affect the total particle concentration in the
598 air (Casquero-Vera et al., 2020).

599 Fig. 7 also demonstrates that diurnal pattern was different, revealing that the particle concentrations at
600 different times of the day were influenced by different sources compared to BC. Almost at all altitudes, the
601 diurnal variation for day 1 and day 2 included a late afternoon peak at 17:00. The particle concentrations
602 increased significantly on the day 3, especially during the first and second samplings before the change to
603 lower concentrations. The samplings for the first two days were carried out during the weekend without many
604 activities that produce VOCs, opposite to Monday morning, when the normal working activities close to
605 sampling area were going-on.

606 In contrast to the pattern of total particle numbers, the daily average of BC concentration during the
607 measurement time period was increased at higher altitudes (Supplemental Table S12), indicating that BC
608 pollutant was distributed from different areas. These trends agree well with the earlier studies (Tripathi et al.,
609 2007). Figure 7 shows that BC diurnal pattern was similar with that of total particle numbers, except on day
610 2 when BC concentration decreased significantly at 13.30, excluding the altitude of 200 m. However, BC
611 concentration increased again at 17.00 most likely due to e.g. sauna heating and air mixing following long-
612 range transport from different areas.

613 During the measurement time, BC at high altitudes 400 m and total particle numbers at all altitudes (100 –
614 400 m) showed diurnal cycle with peak observed on Monday morning at 09:00 am, possible due to morning
615 traffic, and/or to wind-driven pollution transport as suggested by previous studies (Bonasoni et al., 2010;
616 Sandeep et al., 2022). The high BC concentration at high altitude, especially at 400 m, was mostly caused by
617 long-range transport and the atmospheric boundary layer height as discussed earlier, and BC and also other
618 particles contributed to the total particle numbers.

619 **4. Conclusions**

620 An aerial drone carrying the reliable and versatile miniaturized air sampling systems SPME Arrow and ITEX
621 and portable BC and CPC devices was successfully used for the collection of air samples. Up to 48 VOCs
622 were detected in gas and particle phase samples, and their distribution at the altitude from 50 to 400 m was
623 studied. Some differences between VOC compositions at the altitude 50 and 400 m could be explained by
624 the different sources of the VOC emissions. The compounds that most probably originate from the same
625 source had a linear correlation, as well as the compounds that were present both in gas and particle phase
626 samples. The capability of ITEX sampler, furnished with filter accessory for the collection of gas phase



627 samples, was evaluated by comparing it with SPME Arrow sampling resulting in high agreement especially
628 for polar compounds with recoveries up to 99%. In contrast, non-polar compounds gave low recoveries due
629 to the *like dissolve like* rule meaning that non-polar compounds might be adsorbed to the non-polar PTFE
630 filter of the ITEX sampling system.

631 The portable CPC gave comparable results with those obtained by the conventional reference CPC
632 instruments at the SMEAR II Station, opposite to the portable BC device that was affected by drone's vertical
633 and horizontal movements. The total particle number and BC gave similar diurnal pattern, indicating that
634 they were correlated. The pattern was observed during the weekend. The highest concentrations were found
635 during times with human activities. The distribution was also similar to VOCs that were produced by
636 anthropogenic sources and found in high altitude samples, since the wind most probably carried the VOCs
637 from other sites. For spatial distribution pattern, BC concentrations were increased at higher altitudes due to
638 long-range transport and the atmospheric boundary layer height. The total particle numbers, affected by the
639 similar factors, varied more depending on the sources. This can be explained by the different VOCs that
640 contributed to the particle formations, and the particle sizes measured by the portable CPC and BC monitors.

641 Overall, our study work described a drone equipped with miniaturized air sampling techniques, SPME Arrow
642 and ITEX together with portable BC and CPC devices were for the collection of atmospheric VOCs and for
643 the measurement of BC and total number of particles at high altitudes. To further improve the reliability of
644 the results in the future, a portable BC monitor that includes a better electronic model and the possibility to
645 adjust the device position in the drone are needed.

646 **Author contributions.** EDP, JR-J, JH, KH, MJ, TP and M-LR designed the experiments. EDP, AT, MS,
647 JR-J carried out the experiments. JR-J performed the statistical analysis. JH, JK and KL were responsible
648 for CPC and BC hardware, software and reference data. EDP, JR-J, KL, KH, TP and M-LR prepared the
649 manuscript with contributions from other co-authors.

650

651 **Declaration of competing Interest.** One of the (co-)authors is a member of the editorial board of
652 *Atmospheric Chemistry and Physics*. The peer-review process was guided by an independent editor, and the
653 authors have also no other competing interests to declare.

654 **Acknowledgments.** Financial support was provided by the Jane and Aatos Erkkö Foundation and Academy
655 of Finland (ACCC flagship "Finnish Research Flagship" grant no. 337549). CTC Analytics AG (Zwingen,



656 Switzerland) and BGB Analytik AG (Zürich, Switzerland) are thanked for the cooperation. Tapio Elomaa is
657 also acknowledged for the fruitful discussion especially about Black Carbon (BC) and Condensation Particle
658 Counters (CPCs). In addition, we also thank the staff of the SMEAR II Station, Hyytiälä, for the valuable
659 help.

660 References

- 661 Ahlberg, E., Falk, J., Eriksson, A., Holst, T., Brune, W.H., Kristensson, A., Roldin, P., Svenningsson, B., 2017.
662 Secondary organic aerosol from VOC mixtures in an oxidation flow reactor. *Atmos. Environ.* 161, 210–220.
663 <https://doi.org/10.1016/j.atmosenv.2017.05.005>
- 664 Almeida, J., Schobesberger, S., Kürten, A., Ortega, I.K., Kupiainen-Määttä, O., Praplan, A.P., Adamov, A., Amorim,
665 A., Bianchi, F., Breitenlechner, M., David, A., Dommen, J., Donahue, N.M., Downard, A., Dunne, E., Duplissy,
666 J., Ehrhart, S., Flagan, R.C., Franchin, A., Guida, R., Hakala, J., Hansel, A., Heinritzi, M., Henschel, H.,
667 Jokinen, T., Junninen, H., Kajos, M., Kangasluoma, J., Keskinen, H., Kupc, A., Kurtén, T., Kvashin, A.N.,
668 Laaksonen, A., Lehtipalo, K., Leiminger, M., Leppä, J., Loukonen, V., Makhmutov, V., Mathot, S., McGrath,
669 M.J., Nieminen, T., Olenius, T., Onnela, A., Petäjä, T., Riccobono, F., Riipinen, I., Rissanen, M., Rondo, L.,
670 Ruuskanen, T., Santos, F.D., Sarnela, N., Schallhart, S., Schnitzhofer, R., Seinfeld, J.H., Simon, M., Sipilä, M.,
671 Stozhkov, Y., Stratmann, F., Tomé, A., Tröstl, J., Tsagkogeorgas, G., Vaattovaara, P., Viisanen, Y., Virtanen,
672 A., Vrtala, A., Wagner, P.E., Weingartner, E., Wex, H., Williamson, C., Wimmer, D., Ye, P., Yli-Juuti, T.,
673 Carslaw, K.S., Kulmala, M., Curtius, J., Baltensperger, U., Worsnop, D.R., Vehkamäki, H., Kirkby, J., 2013.
674 Molecular understanding of sulphuric acid-amine particle nucleation in the atmosphere. *Nature* 502, 359–363.
675 <https://doi.org/10.1038/nature12663>
- 676 Altshuler, A.P., 1993. Production of aldehydes as primary emissions and from secondary atmospheric reactions of
677 alkenes and alkanes during the night and early morning hours. *Atmos. Environ. Part A, Gen. Top.* 27, 21–32.
678 [https://doi.org/10.1016/0960-1686\(93\)90067-9](https://doi.org/10.1016/0960-1686(93)90067-9)
- 679 Anenberg, S.C., Schwartz, J., Shindell, D., Amann, M., Faluvegi, G., Klimont, Z., Janssens-Maenhout, G., Pozzoli,
680 L., van Dingenen, R., Vignati, E., Emberson, L., Muller, N.Z., Jason West, J., Williams, M., Demkine, V.,
681 Kevin Hicks, W., Kuylenstierna, J., Raes, F., Ramanathan, V., 2012. Global air quality and health co-benefits of
682 mitigating near-term climate change through methane and black carbon emission controls. *Environ. Health*
683 *Perspect.* 120, 831–839. <https://doi.org/10.1289/ehp.1104301>
- 684 Asbach, C., Schmitz, A., Schmidt, F., Monz, C., Todea, A.M., 2017. Intercomparison of a personal CPC and
685 different conventional CPCs. *Aerosol Air Qual. Res.* 17, 1132–1141. <https://doi.org/10.4209/aaqr.2016.10.0460>
- 686 Bonasoni, P., Laj, P., Marinoni, A., Sprenger, M., Angelini, F., Arduini, J., Bonafè, U., Calzolari, F., Colombo, T.,
687 Decesari, S., Di Biagio, C., Di Sarra, A.G., Evangelisti, F., Duchi, R., Facchini, M.C., Fuzzi, S., Gobbi, G.P.,
688 Maione, M., Panday, A., Roccatò, F., Sellegri, K., Venzac, H., Verza, G.P., Villani, P., Vuilleumoz, E.,
689 Cristofanelli, P., 2010. Atmospheric Brown Clouds in the Himalayas: First two years of continuous
690 observations at the Nepal Climate Observatory-Pyramid (5079 m). *Atmos. Chem. Phys.* 10, 7515–7531.
691 <https://doi.org/10.5194/acp-10-7515-2010>
- 692 Bonn, B., von Kuhlmann, R., Lawrence, M.G., 2004. High contribution of biogenic hydroperoxides to secondary
693 organic aerosol formation. *Geophys. Res. Lett.* 31, 1–4. <https://doi.org/10.1029/2003GL019172>
- 694 Boylstein, R., Piacitelli, C., Grote, A., Kanwal, R., Kullman, G., Kreiss, K., 2006. Diacetyl emissions and airborne
695 dust from butter flavorings used in microwave popcorn production. *J. Occup. Environ. Hyg.* 3, 530–535.
696 <https://doi.org/10.1080/15459620600909708>
- 697 Brasseur, G.P., Orlando, J.J., Tyndall, G.S., 1999. *Atmospheric Chemistry and Global Change*. Oxford University
698 Press, New York.



- 699 Buzorius, G., Rannik, Ü., Mäkelä, J.M., Vesala, T., Kulmala, M., 1998. Vertical aerosol particle fluxes measured by
700 eddy covariance technique using condensational particle counter. *J. Aerosol Sci.* 29, 157–171.
701 [https://doi.org/10.1016/S0021-8502\(97\)00458-8](https://doi.org/10.1016/S0021-8502(97)00458-8)
- 702 Camredon, M., Aumont, B., Lee-Taylor, J., Madronich, S., 2007. The SOA/VOC/NO_x system: an explicit model of
703 secondary organic aerosol formation, *Atmos. Chem. Phys.*
- 704 Carnerero, C., Pérez, N., Reche, C., Ealo, M., Titos, G., Lee, H.K., Eun, H.R., Park, Y.H., Dada, L., Paasonen, P.,
705 Kerminen, V.M., Mantilla, E., Escudero, M., Gómez-Moreno, F.J., Alonso-Blanco, E., Coz, E., Saiz-Lopez, A.,
706 Temime-Roussel, B., Marchand, N., Beddows, D.C.S., Harrison, R.M., Petäjä, T., Kulmala, M., Ahn, K.H.,
707 Alastuey, A., Querol, X., 2018. Vertical and horizontal distribution of regional new particle formation events in
708 Madrid. *Atmos. Chem. Phys.* 18, 16601–16618. <https://doi.org/10.5194/acp-18-16601-2018>
- 709 Casquero-Vera, J.A., Lyamani, H., Dada, L., Hakala, S., Paasonen, P., Román, R., Fraile, R., Petäjä, T., Olmo-Reyes,
710 F.J., Alados-Arboledas, L., 2020. New particle formation at urban and high-altitude remote sites in the south-
711 eastern Iberian Peninsula. *Atmos. Chem. Phys.* 20, 14253–14271. <https://doi.org/10.5194/acp-20-14253-2020>
- 712 Chen, J., Jiang, S., Liu, Y.R., Huang, T., Wang, C.Y., Miao, S.K., Wang, Z.Q., Zhang, Y., Huang, W., 2017.
713 Interaction of oxalic acid with dimethylamine and its atmospheric implications. *RSC Adv.* 7, 6374–6388.
714 <https://doi.org/10.1039/c6ra27945g>
- 715 Chen, J., Scircle, A., Black, O., Cizdziel, J. V., Watson, N., Wevill, D., Zhou, Y., 2018. On the use of multicopters
716 for sampling and analysis of volatile organic compounds in the air by adsorption/thermal desorption GC-MS.
717 *Air Qual. Atmos. Heal.* 11, 835–842. <https://doi.org/10.1007/s11869-018-0588-y>
- 718 Chen, T., Ge, Y., Liu, Y., He, H., 2022. N-nitration of secondary aliphatic amines in the particle phase. *Chemosphere*
719 293, 133639. <https://doi.org/10.1016/j.chemosphere.2022.133639>
- 720 Correa, S.M., Arbilla, G., Marques, M.R.C., Oliveira, K.M.P.G., 2012. The impact of BTEX emissions from gas
721 stations into the atmosphere. *Atmos. Pollut. Res.* 3, 163–169. <https://doi.org/10.5094/APR.2012.016>
- 722 De Haan, D.O., Hawkins, L.N., Kononenko, J.A., Turley, J.J., Corrigan, A.L., Tolbert, M.A., Jimenez, J.L., 2011.
723 Formation of nitrogen-containing oligomers by methylglyoxal and amines in simulated evaporating cloud
724 droplets. *Environ. Sci. Technol.* 45, 984–991. <https://doi.org/10.1021/es102933x>
- 725 Dehghani, M., Fazlzadeh, M., Sorooshian, A., Tabatabaee, H.R., Miri, M., Baghani, A.N., Delikhoon, M., Mahvi,
726 A.H., Rashidi, M., 2018. Characteristics and health effects of BTEX in a hot spot for urban pollution.
727 *Ecotoxicol. Environ. Saf.* 155, 133–143. <https://doi.org/10.1016/j.ecoenv.2018.02.065>
- 728 Dou, J., Lin, P., Kuang, B.Y., Yu, J.Z., 2015. Reactive oxygen species production mediated by humic-like substances
729 in atmospheric aerosols: Enhancement effects by pyridine, imidazole, and their derivatives. *Environ. Sci.*
730 *Technol.* 49, 6457–6465. <https://doi.org/10.1021/es5059378>
- 731 Dumka, U.C., Moorthy, K.K., Kumar, R., Hegde, P., Sagar, R., Pant, P., Singh, N., Babu, S.S., 2010. Characteristics
732 of aerosol black carbon mass concentration over a high altitude location in the Central Himalayas from multi-
733 year measurements. *Atmos. Res.* 96, 510–521. <https://doi.org/10.1016/j.atmosres.2009.12.010>
- 734 Elomaa, T., 2022. Mustan hiilen mittaus suodatinpohjaisilla sensoreilla. University of Helsinki.
- 735 Fermo, P., Artíñano, B., De Gennaro, G., Pantaleo, A.M., Parente, A., Battaglia, F., Colicino, E., Di Tanna, G.,
736 Goncalves da Silva Junior, A., Pereira, I.G., Garcia, G.S., Garcia Goncalves, L.M., Comite, V., Miani, A., 2021.
737 Improving indoor air quality through an air purifier able to reduce aerosol particulate matter (PM) and volatile
738 organic compounds (VOCs): Experimental results. *Environ. Res.* 197, 1–8.
739 <https://doi.org/10.1016/j.envres.2021.111131>
- 740 Fu, P., Kawamura, K., Usukura, K., Miura, K., 2013. Dicarboxylic acids, ketocarboxylic acids and glyoxal in the
741 marine aerosols collected during a round-the-world cruise. *Mar. Chem.* 148, 22–32.



- 742 <https://doi.org/10.1016/j.marchem.2012.11.002>
- 743 Ge, X., Wexler, A.S., Clegg, S.L., 2011. Atmospheric amines - Part I. A review. *Atmos. Environ.* 45, 524–546.
744 <https://doi.org/10.1016/j.atmosenv.2010.10.012>
- 745 Hari, P., Kulmala, M., 2005. Station for Measuring Ecosystem-Atmosphere Relations (SMEAR II). *Boreal Environ.*
746 *Res.* 10, 315–322.
- 747 Helin, A., Rönkkö, T., Parshintsev, J., Hartonen, K., Schilling, B., Läubli, T., Riekkola, M.L., 2015. Solid phase
748 microextraction Arrow for the sampling of volatile amines in wastewater and atmosphere. *J. Chromatogr. A*
749 1426, 56–63. <https://doi.org/10.1016/j.chroma.2015.11.061>
- 750 Hemmilä, M., 2020. Chemical Characterisation of Boreal Forest Air with Chromatographic Techniques. University
751 of Helsinki, Helsinki.
- 752 Hemmilä, M., Hellén, H., Virkkula, A., Makkonen, U., Praplan, A.P., Kontkanen, J., Ahonen, L., Kulmala, M.,
753 Hakola, H., 2018. Amines in boreal forest air at SMEAR II station in Finland. *Atmos. Chem. Phys.* 18, 6367–
754 6380. <https://doi.org/10.5194/acp-18-6367-2018>
- 755 Hienola, A.I., Pietikäinen, J.P., Jacob, D., Pozdun, R., Petäjä, T., Hyvärinen, A.P., Sogacheva, L., Kerminen, V.M.,
756 Kulmala, M., Laaksonen, A., 2013. Black carbon concentration and deposition estimations in Finland by the
757 regional aerosol-climate model REMO-HAM. *Atmos. Chem. Phys.* 13, 4033–4055. <https://doi.org/10.5194/acp-13-4033-2013>
- 759 Hoeben, W.F.L.M., Beckers, F.J.C.M., Pemen, A.J.M., Van Heesch, E.J.M., Kling, W.L., 2012. Oxidative
760 degradation of toluene and limonene in air by pulsed corona technology. *J. Phys. D. Appl. Phys.* 45.
761 <https://doi.org/10.1088/0022-3727/45/5/055202>
- 762 Hyvärinen, A.P., Kolmonen, P., Kerminen, V.M., Virkkula, A., Leskinen, A., Komppula, M., Hatakka, J., Burkhart,
763 J., Stohl, A., Aalto, P., Kulmala, M., Lehtinen, K.E.J., Viisanen, Y., Lihavainen, H., 2011. Aerosol black carbon
764 at five background measurement sites over Finland, a gateway to the Arctic. *Atmos. Environ.* 45, 4042–4050.
765 <https://doi.org/10.1016/j.atmosenv.2011.04.026>
- 766 Isidorov, V.A., Pirožnikow, E., Spirina, V.L., Vasyanin, A.N., Kulakova, S.A., Abdulmanova, I.F., Zaitsev, A.A.,
767 2022. Emission of volatile organic compounds by plants on the floor of boreal and mid-latitude forests. *J.*
768 *Atmos. Chem.* 79, 153–166. <https://doi.org/10.1007/s10874-022-09434-3>
- 769 Jacobson, M.Z., 2010. Short-term effects of controlling fossil-fuel soot, biofuel soot and gases, and methane on
770 climate, Arctic ice, and air pollution health. *J. Geophys. Res. Atmos.* 115.
771 <https://doi.org/10.1029/2009JD013795>
- 772 Jang, M., Kamens, R.M., 2001. Atmospheric secondary aerosol formation by heterogeneous reactions of aldehydes in
773 the presence of a sulfuric acid aerosol catalyst. *Environ. Sci. Technol.* 35, 4758–4766.
774 <https://doi.org/10.1021/es010790s>
- 775 Junninen, H., Lauri, A., Keronen, P., Aalto, P., Hiltunen, V., Hari, P., Kulmala, M., 2009. Smart-SMEAR: On-line
776 data exploration and visualization tool for SMEAR stations. *Boreal Environ. Res.* 14, 447–457.
- 777 Kamens, R.M., Zhang, H., Chen, E.H., Zhou, Y., Parikh, H.M., Wilson, R.L., Galloway, K.E., Rosen, E.P., 2011.
778 Secondary organic aerosol formation from toluene in an atmospheric hydrocarbon mixture: Water and particle
779 seed effects. *Atmos. Environ.* 45, 2324–2334. <https://doi.org/10.1016/j.atmosenv.2010.11.007>
- 780 Kanakidou, M., Seinfeld, J.H., Pandis, S.N., Barnes, I., Dentener, F.J., Facchini, M.C., Van Dingenen, R., Ervens, B.,
781 Nenes, A., Nielsen, C.J., Swietlicki, E., Putaud, J.P., Balkanski, Y., Fuzzi, S., Horth, J., Moortgat, G.K.,
782 Winterhalter, R., Myhre, C.E.L., Tsigaridis, K., Vignati, E., Stephanou, E.G., Wilson, J., 2005. Organic aerosol
783 and global climate modelling: A review. *Atmos. Chem. Phys.* 5, 1053–1123. <https://doi.org/10.5194/acp-5-1053-2005>
784



- 785 Kangasluoma, J., Attoui, M., 2019. Review of sub-3 nm condensation particle counters, calibrations, and cluster
786 generation methods. *Aerosol Sci. Technol.* 53, 1277–1310. <https://doi.org/10.1080/02786826.2019.1654084>
- 787 Karlberg, A. -T, Magnusson, K., Nilsson, U., 1992. Air oxidation of d-limonene (the citrus solvent) creates potent
788 allergens. *Contact Dermatitis* 26, 332–340. <https://doi.org/10.1111/j.1600-0536.1992.tb00129.x>
- 789 Kawamura, K., Sakaguchi, F., 1999. Acids Were Detected in the Sample3S). With a Concentration Range of. *North*
790 *104*, 3501–3509.
- 791 Khare, P., Kumar, N., Kumari, K.M., Srivastava, S.S., 1999. Atmospheric formic acid and acetic acids : an overview.
792 *Rev. Geophys.* 227–248.
- 793 Kieloaho, A., 2017. Alkyl Amines in Boreal Forest and Urban Area.
- 794 Kim, H., Park, Y., Kim, W., Eun, H., 2018. Vertical Aerosol Distribution and Flux Measurement in the Planetary
795 Boundary Layer Using Drone *14*, 35–40.
- 796 Kim, S.H., Kirakosyan, A., Choi, J., Kim, J.H., 2017. Detection of volatile organic compounds (VOCs), aliphatic
797 amines, using highly fluorescent organic-inorganic hybrid perovskite nanoparticles. *Dye. Pigment.* 147, 1–5.
798 <https://doi.org/10.1016/j.dyepig.2017.07.066>
- 799 Kim, S.J., Lee, J.Y., Choi, Y.S., Sung, J.M., Jang, H.W., 2020. Comparison of different types of SPME arrow
800 sorbents to analyze volatile compounds in cirsium setidens nakai. *Foods* 9.
801 <https://doi.org/10.3390/foods9060785>
- 802 Kivekäs, N., Sun, J., Zhan, M., Kerminen, V., Hyvärinen, A., Komppula, M., Viisanen, Y., Hong, N., Zhang, Y.,
803 Kulmala, M., Zhang, X., Lihavainen, H., 2009. Long term particle size distribution measurements at Mount
804 Waliguan, a high-altitude site in inland China, *Atmos. Chem. Phys.*
- 805 Kopperi, M., Ruiz-Jiménez, J., Hukkinen, J.I., Riekkola, M.L., 2013. New way to quantify multiple steroidal
806 compounds in wastewater by comprehensive two-dimensional gas chromatography-time-of-flight mass
807 spectrometry. *Anal. Chim. Acta* 761, 217–226. <https://doi.org/10.1016/j.aca.2012.11.059>
- 808 Kristensen, K., Bilde, M., Aalto, P.P., Petäjä, T., Glasius, M., 2016. Denuder/filter sampling of organic acids and
809 organosulfates at urban and boreal forest sites: Gas/particle distribution and possible sampling artifacts. *Atmos.*
810 *Environ.* 130, 36–53. <https://doi.org/10.1016/j.atmosenv.2015.10.046>
- 811 Krueve, A., 2016. Influence of mobile phase, source parameters and source type on electrospray ionization efficiency
812 in negative ion mode. *J. Mass Spectrom.* 51, 596–601. <https://doi.org/10.1002/jms.3790>
- 813 Kulmala, M., Kontkanen, J., Junninen, H., Lehtipalo, K., Manninen, H.E., Nieminen, T., Petäjä, T., Sipilä, M.,
814 Schobesberger, S., Rantala, P., Franchin, A., Jokinen, T., Järvinen, E., Äijälä, M., Kangasluoma, J., Hakala, J.,
815 Aalto, P.P., Paasonen, P., Mikkilä, J., Vanhanen, J., Aalto, J., Hakola, H., Makkonen, U., Ruuskanen, T.,
816 Mauldin, R.L., Duplissy, J., Vehkamäki, H., Bäck, J., Kortelainen, A., Riipinen, I., Kurtén, T., Johnston, M. V.,
817 Smith, J.N., Ehn, M., Mentel, T.F., Lehtinen, K.E.J., Laaksonen, A., Kerminen, V.M., Worsnop, D.R., 2013.
818 Direct observations of atmospheric aerosol nucleation. *Science* (80-.). 339, 943–946.
819 <https://doi.org/10.1126/science.1227385>
- 820 Kulmala, M., Petäjä, T., Ehn, M., Thornton, J., Sipilä, M., Worsnop, D.R., Kerminen, V.M., 2014. Chemistry of
821 atmospheric nucleation: On the recent advances on precursor characterization and atmospheric cluster
822 composition in connection with atmospheric new particle formation. *Annu. Rev. Phys. Chem.* 65, 21–37.
823 <https://doi.org/10.1146/annurev-physchem-040412-110014>
- 824 Kumar, R., Barth, M.C., Nair, V.S., Pfister, G.G., Suresh Babu, S., Satheesh, S.K., Krishna Moorthy, K., Carmichael,
825 G.R., Lu, Z., Streets, D.G., 2015. Sources of black carbon aerosols in South Asia and surrounding regions
826 during the Integrated Campaign for Aerosols, Gases and Radiation Budget (ICARB). *Atmos. Chem. Phys.* 15,
827 5415–5428. <https://doi.org/10.5194/acp-15-5415-2015>



- 828 Lan, H., Hartonen, K., Riekkola, M.L., 2020. Miniaturised air sampling techniques for analysis of volatile organic
829 compounds in air. *TrAC - Trends Anal. Chem.* 126, 115873. <https://doi.org/10.1016/j.trac.2020.115873>
- 830 Lan, H., Holopainen, J., Hartonen, K., Jussila, M., Ritala, M., Riekkola, M.L., 2019a. Fully Automated Online
831 Dynamic In-Tube Extraction for Continuous Sampling of Volatile Organic Compounds in Air. *Anal. Chem.* 91,
832 8507–8515. <https://doi.org/10.1021/acs.analchem.9b01668>
- 833 Lan, H., Ruiz-Jimenez, J., Leleev, Y., Demaria, G., Jussila, M., Hartonen, K., Riekkola, M.-L., 2021. Quantitative
834 analysis and spatial and temporal distribution of volatile organic compounds in atmospheric air by utilizing
835 drone with miniaturized samplers. *Chemosphere* 282, 131024.
836 <https://doi.org/10.1016/j.chemosphere.2021.131024>
- 837 Lan, H., Zhang, W., Smått, J.-H., Koivula, R.T., Hartonen, K., Riekkola, M.-L., 2019b. Selective extraction of
838 aliphatic amines by functionalized mesoporous silica-coated solid phase microextraction Arrow. *Microchim.*
839 *Acta* 186, 412. <https://doi.org/10.1007/s00604-019-3523-5>
- 840 Liu, Y., Monod, A., Tritscher, T., Praplan, A.P., Decarlo, P.F., Temime-Roussel, B., Quivet, E., Marchand, N.,
841 Dommen, J., Baltensperger, U., 2012. Aqueous phase processing of secondary organic aerosol from isoprene
842 photooxidation. *Atmos. Chem. Phys.* 12, 5879–5895. <https://doi.org/10.5194/acp-12-5879-2012>
- 843 McGillen, M.R., Curchod, B.F.E., Chhantyal-Pun, R., Beames, J.M., Watson, N., Khan, M.A.H., McMahon, L.,
844 Shallcross, D.E., Orr-Ewing, A.J., 2017. Criegee Intermediate-Alcohol Reactions, A Potential Source of
845 Functionalized Hydroperoxides in the Atmosphere. *ACS Earth Sp. Chem.* 1, 664–672.
846 <https://doi.org/10.1021/acsearthspacechem.7b00108>
- 847 McMurry, P.H., 2000. The history of condensation nucleus counters. *Aerosol Sci. Technol.* 33, 297–322.
848 <https://doi.org/10.1080/02786820050121512>
- 849 Meena, G.S., Mukherjee, S., Buchunde, P., Safai, P.D., Singla, V., Aslam, M.Y., Sonbawne, S.M., Made, R., Anand,
850 V., Dani, K.K., Pandithurai, G., 2021. Seasonal variability and source apportionment of black carbon over a
851 rural high-altitude and an urban site in western India. *Atmos. Pollut. Res.* 12, 32–45.
852 <https://doi.org/10.1016/j.apr.2020.10.006>
- 853 Moorthy, K.K., Babu, S.S., 2006. Aerosol black carbon over Bay of Bengal observed from an island location, Port
854 Blair: Temporal features and long-range transport. *J. Geophys. Res. Atmos.* 111, 1–10.
855 <https://doi.org/10.1029/2005JD006855>
- 856 Ng, N.L., Kroll, J.H., Chan, A.W.H., Chhabra, P.S., Flagan, R., Seinfeld, J.H., 2007. Pytannia Vzaiemodii Partyzaniv
857 Z Chastynamy Chervonoi Armii Pid Chas Vyzvolennia Pravoberezhnoi Ukrainy V Radians’Kii Istoriohrafii.
858 *Atmos. Chem. Phys.* 7, 3909–3922.
- 859 Nguyen, H.T.H., Takenaka, N., Bandow, H., Maeda, Y., De Oliva, S.T., Botelho, M.M.F., Tavares, T.M., 2001.
860 Atmospheric alcohols and aldehydes concentrations measured in Osaka, Japan and in Sao Paulo, Brazil. *Atmos.*
861 *Environ.* 35, 3075–3083. [https://doi.org/10.1016/S1352-2310\(01\)00136-4](https://doi.org/10.1016/S1352-2310(01)00136-4)
- 862 Oh, H.J., Ma, Y., Kim, J., 2020. Human inhalation exposure to aerosol and health effect: Aerosol monitoring and
863 modelling regional deposited doses. *Int. J. Environ. Res. Public Health* 17, 1–2.
864 <https://doi.org/10.3390/ijerph17061923>
- 865 Olsen, R., Thorud, S., Heresson, M., Øvrebo, S., Lundanes, E., Greibrokk, T., Ellingsen, D.G., Thomassen, Y.,
866 Molander, P., 2007. Determination of the dialdehyde glyoxal in workroom air - Development of personal
867 sampling methodology. *J. Environ. Monit.* 9, 687–694. <https://doi.org/10.1039/b700105n>
- 868 Pan, X.L., Kanaya, Y., Wang, Z.F., Liu, Y., Pochanart, P., Akimoto, H., Sun, Y.L., Dong, H.B., Li, J., Irie, H.,
869 Takigawa, M., 2011. Correlation of black carbon aerosol and carbon monoxide in the high-altitude environment
870 of Mt. Huang in Eastern China. *Atmos. Chem. Phys.* 11, 9735–9747. <https://doi.org/10.5194/acp-11-9735-2011>



- 871 Parshintsev, J., Ruiz-Jimenez, J., Petäjä, T., Hartonen, K., Kulmala, M., Riekkola, M.L., 2011. Comparison of quartz
872 and Teflon filters for simultaneous collection of size-separated ultrafine aerosol particles and gas-phase zero
873 samples. *Anal. Bioanal. Chem.* 400, 3527–3535. <https://doi.org/10.1007/s00216-011-5041-0>
- 874 Parsons, G.E., Buckton, G., Chatham B', S.M., 1992. The use of surface energy and polarity determinations to
875 predict physical stability of non-polar, non-aqueous suspensions, *International Journal of Pharmaceutics*.
- 876 Peng, L., Li, Z., Zhang, G., Bi, X., Hu, W., Tang, M., Wang, X., Peng, P., Sheng, G., 2021. A review of
877 measurement techniques for aerosol effective density. *Sci. Total Environ.* 778, 146248.
878 <https://doi.org/10.1016/j.scitotenv.2021.146248>
- 879 Perez, J.E., Kumar, M., Francisco, J.S., Sinha, A., 2017. Oxygenate-Induced Tuning of Aldehyde-Amine Reactivity
880 and Its Atmospheric Implications. *J. Phys. Chem. A* 121, 1022–1031. <https://doi.org/10.1021/acs.jpca.6b10845>
- 881 Petäjä, T., Laakso, L., Grönholm, T., Launiainen, S., Evele-Peltoniemi, I., Virkkula, A., Leskinen, A., Backman, J.,
882 Manninen, H.E., Sipilä, M., Haapanala, S., Hämeri, K., Vanhala, E., Tuomi, T., Paatero, J., Aurela, M., Hakola,
883 H., Makkonen, U., Hellén, H., Hillamo, R., Vira, J., Prank, M., Sofiev, M., Siitari-Kauppi, M., Laaksonen, A.,
884 lehtinen, K.E.J., Kulmala, M., Viisanen, Y., Kerminen, V.M., 2012. In-situ observations of Eyjafjallajökull ash
885 particles by hot-air balloon. *Atmos. Environ.* 48, 104–112. <https://doi.org/10.1016/j.atmosenv.2011.08.046>
- 886 Petäjä, T., Rannik, Ü., Buzorius, G., Aalto, P., Vesala, T., Kulmala, M., 2001. Deposition Velocities of Ultrafine
887 Particles Into Scots Pine Forest During Nucleation Events. *J. Aerosol Sci.* 32, 143–144.
888 [https://doi.org/10.1016/s0021-8502\(21\)00068-9](https://doi.org/10.1016/s0021-8502(21)00068-9)
- 889 Pusfitasari, E.D., Ruiz-Jimenez, J., Heiskanen, I., Jussila, M., Hartonen, K., Riekkola, M.-L., 2022. Aerial drone
890 furnished with miniaturized versatile air sampling systems for selective collection of nitrogen containing
891 compounds in boreal forest. *Sci. Total Environ.* 808, 152011.
892 <https://doi.org/10.1016/J.SCITOTENV.2021.152011>
- 893 Rajesh, T.A., Ramachandran, S., 2018. Black carbon aerosols over urban and high altitude remote regions:
894 Characteristics and radiative implications. *Atmos. Environ.* 194, 110–122.
895 <https://doi.org/10.1016/j.atmosenv.2018.09.023>
- 896 Rinaldi, M., Decesari, S., Carbone, C., Finessi, E., Fuzzi, S., Ceburnis, D., O'Dowd, C.D., Sciare, J., Burrows, J.P.,
897 Vrekoussis, M., Ervens, B., Tsigaridis, K., Facchini, M.C., 2011. Evidence of a natural marine source of oxalic
898 acid and a possible link to glyoxal. *J. Geophys. Res. Atmos.* 116, 1–12. <https://doi.org/10.1029/2011JD015659>
- 899 Rosado-Reyes, C.M., Francisco, J.S., 2006. Atmospheric oxidation pathways of acetic acid. *J. Phys. Chem. A* 110,
900 4419–4433. <https://doi.org/10.1021/jp0567974>
- 901 Ruiz-Jimenez, J., Zanca, N., Lan, H., Jussila, M., Hartonen, K., Riekkola, M.L., 2019. Aerial drone as a carrier for
902 miniaturized air sampling systems. *J. Chromatogr. A* 1597, 202–208.
903 <https://doi.org/10.1016/j.chroma.2019.04.009>
- 904 Safai, P.D., Kewat, S., Praveen, P.S., Rao, P.S.P., Momin, G.A., Ali, K., Devara, P.C.S., 2007. Seasonal variation of
905 black carbon aerosols over a tropical urban city of Pune, India. *Atmos. Environ.* 41, 2699–2709.
906 <https://doi.org/10.1016/j.atmosenv.2006.11.044>
- 907 Sahli, A., 1992. X ; H ; X 1009–1012.
- 908 Sandeep, K., Panicker, A.S., Gautam, A.S., Beig, G., Gandhi, N., S, S., Shankar, R., Nainwal, H.C., 2022. Black
909 carbon over a high altitude Central Himalayan Glacier: Variability, transport, and radiative impacts. *Environ.*
910 *Res.* 204. <https://doi.org/10.1016/j.envres.2021.112017>
- 911 Sato, K., Ikemori, F., Ramasamy, S., Fushimi, A., Kumagai, K., Iijima, A., Morino, Y., 2021. Four- and five-carbon
912 dicarboxylic acids present in secondary organic aerosol produced from anthropogenic and biogenic volatile
913 organic compounds. *Atmosphere (Basel)*. 12. <https://doi.org/10.3390/atmos12121703>



- 914 Sinclair, V.A., Ritvanen, J., Urbancic, G., Statnaia, I., Batrak, Y., Moisseev, D., Kurppa, M., 2022. Boundary-layer
915 height and surface stability at Hyytiala, Finland, in ERA5 and observations. *Atmos. Meas. Tech.* 15, 3075–
916 3103. <https://doi.org/10.5194/amt-15-3075-2022>
- 917 Takahama, S., Schwartz, R.E., Russell, L.M., MacDonald, A.M., Sharma, S., Leaitch, W.R., 2011. Organic
918 functional groups in aerosol particles from burning and non-burning forest emissions at a high-elevation
919 mountain site. *Atmos. Chem. Phys.* 11, 6367–6386. <https://doi.org/10.5194/acp-11-6367-2011>
- 920 Teich, M., Schmidpott, M., van Pinxteren, D., Chen, J., Herrmann, H., 2020. Separation and quantification of
921 imidazoles in atmospheric particles using LC–Orbitrap-MS. *J. Sep. Sci.* 43, 577–589.
922 <https://doi.org/10.1002/jssc.201900689>
- 923 Tripathi, S.N., Srivastava, A.K., Dey, S., Satheesh, S.K., Krishnamoorthy, K., 2007. The vertical profile of
924 atmospheric heating rate of black carbon aerosols at Kanpur in northern India. *Atmos. Environ.* 41, 6909–6915.
925 <https://doi.org/10.1016/j.atmosenv.2007.06.032>
- 926 Weingartner, E., Saathoff, H., Schnaiter, M., Streit, N., Bitnar, B., Baltensperger, U., 2003. Absorption of light by
927 soot particles: Determination of the absorption coefficient by means of aethalometers. *J. Aerosol Sci.* 34, 1445–
928 1463. [https://doi.org/10.1016/S0021-8502\(03\)00359-8](https://doi.org/10.1016/S0021-8502(03)00359-8)
- 929 Wen, L., Schaefer, T., He, L., Zhang, Y., Sun, X., Ventura, O.N., Herrmann, H., 2021. T- And pH-Dependent
930 Kinetics of the Reactions of $\cdot\text{OH}(\text{aq})$ with Glutaric and Adipic Acid for Atmospheric Aqueous-Phase Chemistry.
931 *ACS Earth Sp. Chem.* 5, 1854–1864. <https://doi.org/10.1021/acsearthspacechem.1c00163>
- 932 Yassaa, N., Brancaleoni, E., Frattoni, M., Ciccioli, P., 2006. Isomeric analysis of BTEXs in the atmosphere using β -
933 cyclodextrin capillary chromatography coupled with thermal desorption and mass spectrometry. *Chemosphere*
934 63, 502–508. <https://doi.org/10.1016/j.chemosphere.2005.08.010>
- 935 Youn, J.-S., Crosbie, E.S. B., Maudlin, L.C., Wang, Z., Sorooshian, A., 2015. Dimethylamine as a major alkyl amine
936 species in particles and cloud water: Observations in semi-arid and coastal regions. *Atmos. Environ.* 122, 250–
937 258. <https://doi.org/doi:10.1016/j.atmosenv.2015.09.061>
- 938 Yu, K., Mitch, W.A., Dai, N., 2017. Nitrosamines and Nitramines in Amine-Based Carbon Dioxide Capture Systems:
939 Fundamentals, Engineering Implications, and Knowledge Gaps. *Environ. Sci. Technol.* 51, 11522–11536.
940 <https://doi.org/10.1021/acs.est.7b02597>
- 941 Zahardis, J., Geddes, S., Petrucci, G.A., 2008. The ozonolysis of primary aliphatic amines in fine particles. *Atmos.*
942 *Chem. Phys.* 8, 1181–1194. <https://doi.org/10.5194/acp-8-1181-2008>
- 943 Zhang, R., Shen, J., Xie, H.-B., Chen, J., Elm, J., 2022. The role of organic acids in new particle formation from
944 methanesulfonic acid and methylamine. *Atmos. Chem. Phys.* 22, 2639–2650.
945 <https://doi.org/doi.org/10.5194/acp-22-2639-2022>
- 946 Zhang, Y., Wang, X., Wen, S., Herrmann, H., Yang, W., Huang, X., Zhang, Z., Huang, Z., He, Q., George, C., 2016.
947 On-road vehicle emissions of glyoxal and methylglyoxal from tunnel tests in urban Guangzhou, China. *Atmos.*
948 *Environ.* 127, 55–60. <https://doi.org/10.1016/j.atmosenv.2015.12.017>
- 949 Zhao, Y.L., Garrison, S.L., Gonzalez, C., Thweatt, W.D., Marquez, M., 2007. N-nitrosation of amines by NO₂ and
950 NO: A theoretical study. *J. Phys. Chem. A* 111, 2200–2205. <https://doi.org/10.1021/jp0677703>
- 951 Ziemann, P.J., Atkinson, R., 2012. Kinetics, products, and mechanisms of secondary organic aerosol formation.
952 *Chem. Soc. Rev.* 41, 6582–6605. <https://doi.org/10.1039/c2cs35122f>
- 953